FOULING REDUCTION VIA AIR BACKPULSING IN DAIRY WASTEWATER MICROFILTRATION

By

Mahsa Ashtari

Bachelor of Science in Chemical Engineering

University of Tehran, Iran, 2014

A thesis

presented to Ryerson University

in partial fulfillment of the

requirements for the degree of

Master of Applied Science

in the Program of

Chemical Engineering

Toronto, Ontario, Canada, 2019

Authors Declaration

I hereby declare that I am the sole author of this thesis. This is a true copy of the thesis, including any required final revisions, as accepted by my examiners.

I authorize Ryerson University to lend this thesis to other institutions or individuals for the purpose of scholarly research.

I further authorize Ryerson University to reproduce this thesis by photocopying or by other means, in total or in part, at the request of other institutions or individuals for the purpose of scholarly research.

I understand that my thesis may be made electronically available to the public.

Abstract

Membrane fouling mitigation in dairy wastewater microfiltration was investigated through air back pulsing. Flat sheet membrane module with pore size of 0.1 µm was used. The model dairy wastewater was prepared by skim milk diluted with distilled water (milk:water = 1:2). The effect of three parameters, including air back pulsing pressure (p_b), back pulsing frequency (f), and back pulsing duration (d) on fouling control was investigated. It was found that high pressures of air in short durations of back pulsing can improve the filtration process and result in higher amounts of permeate. However, it is anticipated that beyond the region of study, very high frequency would not be helpful. Very high frequencies mean short back pulsing durations, and this might result in loss of positive effect of back pulsing. The maximum permeate amount obtained using back pulsing assisted filtration process was 83% higher than the one obtained without back pulsing.

Acknowledgment

I would like to express my sincere gratitude to my supervisor Dr. Huu Doan and my co-supervisor Dr. Ali Lohi for their patient guidance, encouragement and advice throughout my research. I am thankful to have had Dr. Doan as a skilful and knowledgeable professor to supervise me through my progress in this study and provide me with valuable insights every step of the way.

I would like to thank Mr. Ali Hemmati, Mr. Tondar Tajrobehkar and Mr. Daniel Boothe for their technical assistance and all the faculty members and staff in the Department of Chemical Engineering at Ryerson University.

Further, I am grateful to my father and my mother, whom without their emotional support and patience, I would have not been able to complete this work. They cared for me and believed in me even more than I did for myself. Also, I am thankful to my dear friend, Dr. Farzad Nikfar, who provided me with his valuable experience and guidance throughout.

Finally, I would like to acknowledge the National Science and Engineering Council (NSERC) of Canada and the Department of Chemical Engineering at Ryerson University for their financial support on this work.

Table of Contents

List of Tables

List of Figures

Introduction

About 71 percent of earth surface is covered with water; however, only three percent of this amount is freshwater and fit for use to sustain human life. Human population growth coupled with industrialization and urbanization has led to the increased pollution of the existing freshwater resources. Moreover, the rise in earth's average temperature within the last decade, also referred to as the global warming phenomena, has left some regions dry and rainless while other regions receive large amount of precipitation throughout the year and are facing issues such as flooding and massive hurricanes. Supplying purified water to water short areas has been a concern on international agenda since 1970's and currently the treatment of sewage and industrial wastewater is widely accepted strategy to address this concern sustainably and efficiently. (Basile, et al., 2015)

In the recent decades, membrane filtration process has become a significant separation technology in the field of water filtration, providing a favourable alternative to related technologies such as adsorption, extraction, distillation, ion exchangers, and sand filters. Low-energy consumption, continuous separation, easy scale-up, process and plant compactness, simple automation, and no need for chemicals are well-recognized key advantages of membrane processes over conventional separation technologies. (Basile, et al., 2015)

A membrane is a porous selective layer that is capable of separating materials as a function of their physical and chemical properties when a driving force is applied across the membranes. Membrane separation process allows selective and controlled transfer of one species from one bulk phase to another bulk phase. This process relies on differentiation and selectivity between molecular weights and sizes and therefore is a physical separation process. Membrane process can be classified into two groups based on applied transmembrane pressure (TMP) and molecular weight cut off: low-pressure membranes and high-pressure membranes. Ultrafiltration and Microfiltration as low-pressure membranes have pore size ranging from 0.1 µm to 2 nm and Nanofiltration and Reverse Osmosis as high-pressure membranes have pore size ranging from 2nm to < 1 nm. Ultrafiltration and Microfiltration with larger nominal pore sizes

provide high degree removal of suspended solids and macromolecules including viruses and bacteria (Basile, et al., 2015). However, Nanofiltration and Reverse Osmosis provide high quality water for potable reuse and high-purity industrial process water.

A major obstacle toward widespread application of membrane technology in wastewater treatment is membrane fouling. In general, membrane fouling is characterized as increased flow resistance due to pore blocking, cake formation and concentration polarization. (Kim, et al., 2007). Pore blocking and cake formation happens by partial adsorption and/or deposition of the material in the pore space or on the membrane surface. Concentration polarization refers to the emergence of concentration gradients at the membrane/solution interface resulted from selective transfer of some species through the membrane. (Hoek, et al., 2013)

Membrane fouling affects the quality of treated water and ultimately requires membranes to be replaced; which in turn results in higher costs of energy, operation, and maintenance of the treatment plant. To maintain the economic viability of a membrane filtration process, membrane fouling must be kept to a minimum, and therefore, membrane fouling control strategies have been the focus for their practical applications, in recent years.

Large amount of wastewater is produced in dairy processing plants every day. In fact, dairy industries are among the critical polluters with the average of 5.5 liters of wastewater per liter of processed milk (Basile, et al., 2015). Dairy wastewater is composed of diluted milk (lipid, protein and lactose) and cleaning chemicals (acids, alkalis and detergents) and represents a waste of water and nutrients as well as pollution (Zielińska, et al., 2017). Because of high concentrations of organic matter, this wastewater presents high Chemical Oxygen Demand (COD) levels and is generally of dark color and milky/turbid appearance. However, since dairy wastewater does not contain toxic chemicals, in recent years, researchers have shifted their interest in reuse or recycling of dairy wastewater to reduce the consumption of fresh water.

Many studies have been performed on dairy wastewater treatment using membrane technology; however, researchers are still examining both high pressure (i.e., Nanofiltration / Reverse osmosis) and low-pressure (i.e., Ultrafiltration / Microfiltration) membrane techniques. Nanofiltration (NF) and Reverse Osmosis (RO) produce very high-quality permeate (low total organic carbon and conductivity), a large volume of permeate (90–95%) and recovery of lactose

and milk proteins. However, there is a rapid increase in osmotic pressure and flux decline due to fouling in this process. Another problem with NF/RO treatment of dairy wastewater is difficulty of nutrients recovery due to their contamination (lipids, proteins and lactose) by cleaning agents. That is because cleaning chemicals contained in dairy waste water and the nutrients are all retained by NF/RO (Zielińska, et al., 2017).

Microfiltration (MF) and ultrafiltration (UF) yield a high flux of permeate at low transmembrane pressure, which means that these techniques have lower energy costs than NF or RO; however, MF and UF reduce COD poorly and do not collect small solutes like lactose. Therefore, permeate water from MF/UF is not reusable as it contains too much lactose. In most cases, these techniques are used as pre-treatment for recycling of valuable components like milk proteins and reducing RO fouling rate. A system designed with ultrafiltration as pre-treatment prior to reverse osmosis is referred to as Integrated Membrane System (IMS) (Wenten).

With a suitable MF and UF membrane selection at pretreatment stage, lipids and proteins can be concentrated and collected, while small solutes such as lactose, chemicals and salts can easily pass through the membrane. At this stage, the osmotic pressure in retentate compartment will not increase significantly and consequently flux decline can be small by maintaining high sheer stress at membrane surface. The retentate could be then used for algae cultivation to produce biodiesel and biofuel. Considering the high absorption and utilization of nitrogen (N) and phosphorus (P) by algae, the problem of N and P removal from dairy wastewater could be addressed as well (Luo, et al., 2011).

Membrane fouling for the dairy wastewater pre-treatment with ultrafiltration, is mainly composed of casein micelle and whey proteins on the membrane surface or internal membrane pores (Zhanga, et al., 2017).

Many strategies have been proposed by researchers to minimize/remove fouling and to improve permeability. These strategies can be classified into various categories including feed pretreatment, membrane modification, flow manipulation (turbulence promotion, backwashing, gas sparging) and using force fields like electric and ultrasonic fields as means to enhance turbulence and shear stress near the membrane surface. Some of these techniques are currently in use in the industry and the others show promise for the future. (Fouladitajara, et al., 2014).

Pretreatments, including coagulation, adsorption, and pre-oxidation, can in various degrees alleviate the fouling by pre-reacting of additives with the foulants in the feed water. However, adverse effects from the pretreatment are also observed.

In this work, membrane fouling control was investigated using air back pulsing method on flat sheet microfiltration module with pore size of 0.1 µm. A model dairy wastewater, representative of actual wastewater properties, was prepared and used as a feed. The effects of different parameters, including back pulsing air pressure, frequency, and duration, on filtration performance of this type of feed were studied.

A review of previous studies on common physical cleaning methods is presented in chapter one. In chapter two, materials and methods of the current study is thoroughly described, and chapter three presents the results and discusses the observed trends in detail.

Chapter One: Literature Review

A major obstacle toward widespread application of membrane technology in wastewater treatment is membrane fouling. In general, membrane fouling is characterized as reduced permeate flux and increased flow resistance due to pore blocking, cake formation and concentration polarization (Kim, et al., 2007)

Pore blocking, and cake formation happens by the partial adsorption and/or deposition of the material in the pore space or on the membrane surface. Concentration polarization refers to the emergence of concentration gradients at the membrane/solution interface resulted from selective transfer of some species through the membrane. Generally, the cause of concentration polarization is the ability of a membrane to transport some species more readily than the others: the retained species are concentrated at the upstream membrane surface while the concentration of transported species decreases. (Hoek, et al., 2013)

Membrane fouling decrease the efficiency of treatment process and affect the quality of treated water to a point where the membranes need to be replaced. Therefore, the high costs of energy, operation, and maintenance of the treatment plant are matters of question. To maintain the economic viability of a membrane process, membrane fouling must be kept to a minimum, and therefore, practical applications of membrane fouling control strategies have been the focus of several researches in recent years.

Two types of fouling phenomena have been identified for microfiltration and ultrafiltration; the first type is caused by particles larger than membranes pores, which can not pass through the membrane. This fouling, known as filtration-induced particle deposition, occurs as external fouling or cake formation on the top membrane surface and is often reversible and non-adhesive. The reversible fouling can be removed by a strong shear force such as backwashing. The second type is caused by the adsorption of the particles (e.g., humic substances, proteins, etc.) on the membrane surface or in the pores. This attachment depends on the specific intermolecular interactions between the particles and the membrane and is usually irreversible and adhesive. Irreversible fouling can not be removed by physical cleaning

methods and may require chemical cleaning for the permeate flux to be fully recovered. (Akhondi, et al., 2014)

Many strategies have been proposed by researchers to minimize/remove fouling and to improve permeability. These strategies can be classified into various categories including feed pretreatment, membrane modification, flow manipulation (turbulence promotion, backwashing, gas sparging) and use of force fields like electric and ultrasonic fields as means to enhance turbulence and shear stress near the membrane surface. Some of these techniques are currently in use in the industry and others show promise for the future. (Fouladitajara, et al., 2014).

Pretreatments, including coagulation, adsorption, and pre-oxidation, can in various degrees alleviate the fouling by pre-reacting of additives with the foulants in the feed water. However, adverse effects from the pretreatment are also observed.

1.1 Backwashing

Backwashing and air sparging are common physical approaches in low pressure membrane filtration systems which can effectively attain fouling reduction (Gao, et al., 2011; Akhondi, et al., 2014)

Backwashing consist of a periodic reversed flux of permeate flowing back through the membrane. Backwashing process consists of two steps. The first step consists of the detachment of fouling cake layer from the membrane surface by a reversed flow of permeate or deionized water pumped towards the retentate (concentrate) compartment. The first step is most effective when backwashing is performed in very short duration (less than 1 second) and it is called backshock. The second step consists of rinsing the retentate compartment where the detached material has accumulated (Serraa, et al., 1999)

Although essential to recover membrane permeate flux, there are certain drawbacks to this technique. The backwash requires the filtration to be stopped and some permeate to be consumed; therefore, leading to a reduction in the process productivity (Cui, et al., 2003). The fouling cake sometimes serves as another screening layer to protect the membrane from internal fouling by macromolecular components. Thus, frequent backwash could provide additional opportunities for macromolecules to enter the membrane pores (Akhondi, et al., 2014; Cabassuda, et al., 2001).

Many studies have been conducted on the mechanisms through which backwashing efficiency can be improved. Among those are: addition of gas or chemical agents to backwashing water or permeate (chemically enhanced backwashing techniques).

Fujioka, et al. (2015) evaluated the use of ozonated water to backwash ceramic membrane used in municipal wastewater treatment. Due to the high fouling potential associated with raw wastewater, the use of direct membrane filtration is often accompanied with the intensive use of chemical agents such as sodium hydroxide, hypochlorite and hydrochloric acid. A promising alternative to these chemicals is ozone, which can be generated on-site and is completely decomposed to oxygen after being used for oxidation and disinfection. The ceramic MF with a nominal pore size of 0.2 μm was used. Conventional backwashing was conducted using RO filtered water without ozonation (i.e., ozone-free water) and ozonated backwashing was performed using tap water filtered with reverse osmosis (RO) cartridge (Merck Millipore, Australia) and induced with Ozone. Direct MF filtration of municipal wastewater led to a considerable increase in TMP. Membrane fouling in the initial stage of each filtration cycle was predominantly governed by cake formation, whilst cake layer compaction appeared in the later stage. Backwashing with ozone-free water could not fully recover the membrane permeability, leading to a notable increase in TMP after each filtration cycle. Almost complete removal of the fouling resistance was obtained by applying backwashing with ozonated water for an extended period (i.e., 2.5 min). An extended backwashing time (e.g., 3.5 min) was sufficient to reduce in the fouling resistance of a heavily fouled membrane to the clean membrane condition. This suggests that backwashing with ozonated water can be employed to filtrate waters with high fouling potential.

The efficiency of back washing can be further improved when coupled with flushing or rinsing step. Rinsing or flushing consist of accelerated feed stream flowing across the membrane in order to carry away the accumulates (Bessiere, et al., 2009). This method if undertaken before the formation of foulant deposit, has proven efficient in reducing particle deposition on the fibre by keeping the potential fouling materials in the dispersed phase. Efficiency of rinsing is greatly improved using air. In such case, during rinsing the air is injected in to feed compartment and acts as a piston, flushing out the major part of the compartment. The rinse time to recover the

initial permeate flux inside the module can be reduced by up to 70% in the presence of air (Li, et al., 1998).

Bessiere, et al. (2009) aimed to improve the backwash efficiency and proposed an alternative way to remove accumulated material to achieve a more sustainable method of operating the filtration cycle. They studied hollow fiber membrane fouling mitigation during dead-end filtration of drinking water by coupling two procedures, 1) rinsing to reduce the material accumulation prior to the formation of deposit and 2) air-assisted back wash (AABW) to remove the deposit and carry them away from membrane surface. The feed used in this study was natural surface water. The results of the coupled process and the conventional single phase backwash were compared. For the two operating conditions, the fouling rates were compared, and then the energy consumtions were determined. The evolution of the normalised initial permeability (defined as the ratio of the permeability at the beginning of a cycle after cleaning of the fouled membrane, Lp_{beg}Lp$_{\mathrm{beg}}$, over the initial permeability of the fresh membrane, L_{p0}L$_{\mathrm{p0}}$) is presented in Figure 1 as a function of the net permeate production for the two backwashes procedures investigated and for the combination of rinsing and AABW.

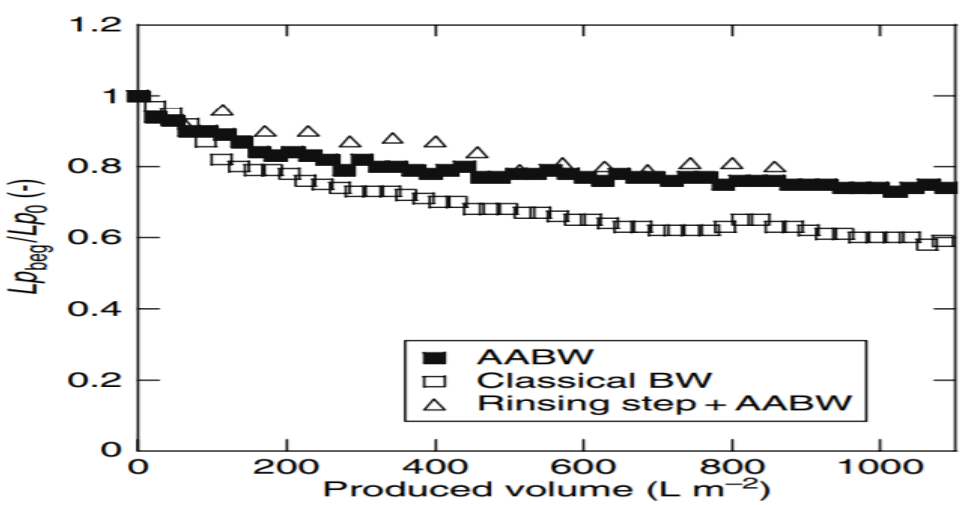

Figure 1- Effect of hydraulic action on the evolution of the normalized initial permeability during the production of permeate from the Canal du Midi. (Bessiere, et al., 2009)

A noticeable decrease in the normalized initial permeability was observed no matter which cleaning procedure was employed; however, the initial decline in the normalized initial

permeability was less pronounced when air was used during the cleaning cycle. No significant difference was observed between AABW and the combined rinsing step + AABW cycle.

Complementary information was provided by examining the fouling rate, defined as the increase in TMP with time (dTMP/dt), as this parameter is linked to the accumulation of material during a filtration cycle, and therefore, to the residual particulate fouling. Its evolution with permeate volume for the three different procedures investigated is shown in Figure 2.

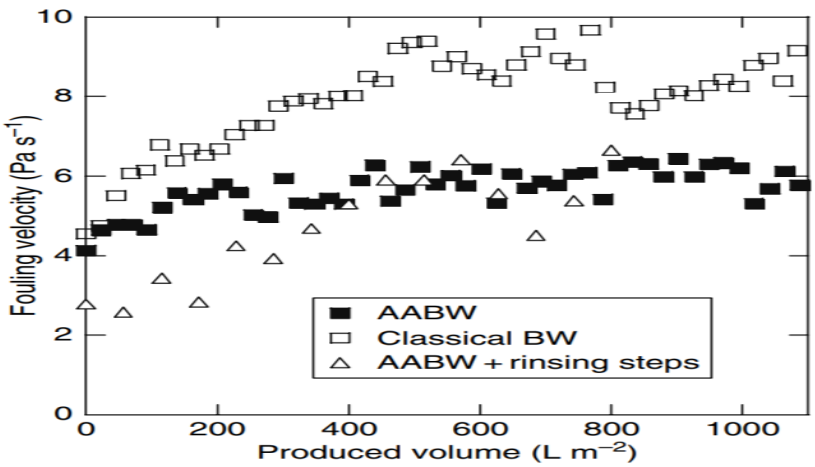

Figure 2- Effect of hydraulic action on the evolution of fouling rate for each filtration cycle. (Bessiere, et al., 2009)

The fouling rate was clearly influenced by the backwash procedure as there is an obvious difference in fouling rate in three different operating conditions with AAWD being the most effective.

Figure 3 shows the direct consequences of the different hydraulic actions, including Back washing, Air assisted back washing (AAWB) and rinsing step + AABW, in terms of the total energy consumption as a function of the net permeate production.

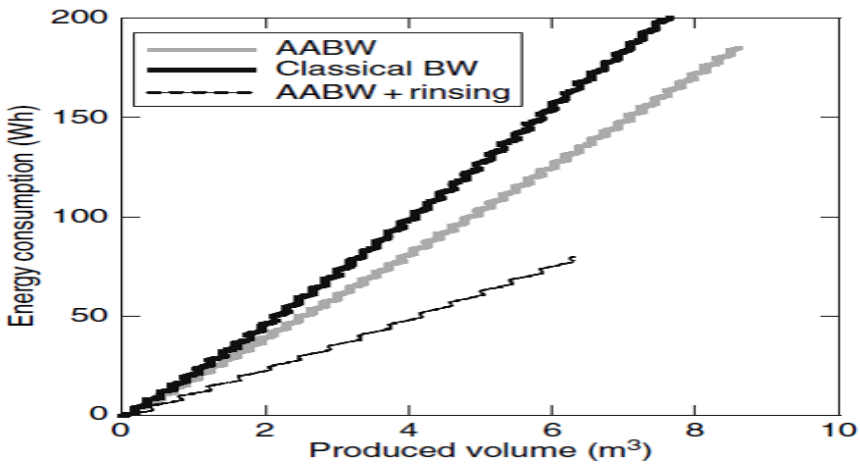

Figure 3- Effect of hydraulic actions employed on energy consumption for the same net permeate production. (Bessiere, et al., 2009)

The results confirmed that backwash with two-phase flow greatly improves the removal of particulates and this has direct consequences on the degree of fouling. Furthermore, by coupling the rinsing step and the AABW procedure the fouling was significantly reduced leading to energy savings of 65%, as compared to a conventional backwash, without air injection (Bessiere, et al., 2009).

Abdelrasoul, et al. (2018) investigated the effect of water and injected air back washing on fouling cleaning for flux restoration in ultrafiltration of simulated latex effluent. Backwashing water, forward air flushing, or combination of air and water was used to remove the particles blocking the membrane pores on the feed side in order to reduce the influence of fouling. Polycarbonate and Polysulfone flat membranes with uniform pore size of 0.05 µm and molecular weight cut of 60,000 were used under a constant feed flow rate and cross-flow mode. Influences of backwashing frequency, duration, and intensity on the efficiency of membrane cleaning were examined and the optimal backwashing scenario and its optimal operational conditions were obtained. Results showed that crossflow water backwashing was effective in terms of cleaning membrane fouling and restoring 60% and 52% of the permeate flux for the uniform and the non-uniform membranes, respectively. Alternatively, air flushing restored the permeate flux by 28% and 19% for the uniform and the non-uniform membranes, respectively. Resutls reflected that at the same duration of backwashing, water backwash could remove solid particles twice as much that of air flushing. These experimental results indicated that the shear force of the air stream could remove fouling materials on the membrane surface but did little to reduce the fouling

within the membrane pores. The combination of air and water backwashing was the most effective method. Overall, the permeate flux was restored by 75% and 63% for the uniform and the non-uniform membranes, respectively. However, the combined air and water backwashing had a negative effect on the membrane's life time and the mechanical strength of the membrane since the membranes were torn up during the second filtration cycle. (Abdelrasoul, et al., 2018)

1.2 Air sparging

Fouling reduction and filtration improvement can also be achieved through use of air as a secondary flow. Air has for a long time been used to increase the efficiency of sand-filter washing. Recent studies indicate that the injection of air during membrane filtration results in an increase in the permeate flux. It is suggested that the injected gas could disrupt the concentration polarization layer by inducing shear stress and providing enough mass transferring motion to avoid the foulants from compacting on the membrane surface (Fouladitajara, et al., 2014; Ye, et al., 2014)

The purpose of the air might be different. It can be used to detach and carry away the particles deposit by a gas back pulsing such as in the Memcor process. In this case the gas under pressure sequentially flows inside the membrane pores from the permeate to the concentrate compartment. Alternatively, it is used to prevent or to limit the formation of fouling cake or concentration polarization. The gas is then injected in the concentrate compartment during filtration or during rinsing phases. This concept, called air sparging, was first proposed by Hitachi, Ltd. in electrodialysis systems in 1986. (Cabassuda, et al., 2001)

Air sparging may be applied intermittently or continuously and its effectiveness is reported to be more pronounced in low cross-flow velocity operations (Cui, et al., 2003).

Influence of a gas/liquid two-phase flow on ultrafiltration and microfiltration performance was studied by Mercier-Bonin, et al. (2000). Air was injected into the feed flow in order to improve filtration performance (flux, energy consumption) of a ceramic flat sheet membrane during crossflow filtration of a commercially available baker's yeast suspension, commonly found in the biotechnology industry. The effect of different operating parameters (gas flowrate, liquid flowrate, feed concentration) was evaluated with horizontally and vertically installed UF or MF membranes. The objective of this study was to verify the effect of the two-phase flow on the

filtration performance and to overcome the drawbacks of conventional steady crossflow filtration with a high axial pressure drop, and hence, non-uniform transmembrane pressure and a significant energy loss in turbulent flow. Steady and unsteady conditions are referred to as two-phase flow and single-phase flow filtration for the purpose of this study. To this end, the effects of the operating parameters (liquid and gas flowrates, feed concentration) and the membrane orientation were investigated and quantified. The results indicated that for both steady and unsteady condition the flux declined rapidly for about 15 minutes and then a gradual decline of the flux was observed. After about 300 minutes a steady flux of J_f was reached. This steady state permeate flux J_f was used for comparison of the results of different conditions. J_f is indicative of the hydrodynamic conditions when obtained under unsteady and steady conditions with the same liquid flowrate. Unsteadiness of two-phase flow was found to enhance the permeate flux by a factor of nearly 4 compared with single-phase steady microfiltration. Such observations prove the primary role played by the fluid instabilities on the significant reduction of external fouling. However, fluid instabilities do not appear to solve the important problem of adsorption and membrane clogging by colloids and macromolecular material likely present in more complex biological suspensions.

It was observed that the two-phase flow unsteadiness was unable to fully disrupt a previously built-up deposit, even with increasing proportions of injected gas. This suggested that an adhesive cake, which was formed during the steady single-phase filtration, could not be easily removed by an on–off gas injecting process. Extracellular compounds (mainly proteins) with strong physicochemical and mechanical interactions also contributed to the formation of fouling. This result indicates that for an optimal filtration efficiency where cake formation was expected to be the main mechanism for flux decline, two-phase flow unsteadiness had to be started at the very beginning of the filtration operation.

Under the overall experimental conditions, the energy consumption per unit volume of permeate was found to be considerably lower in two-phase flow than in single-phase steady flow. For a given specific energy, the permeate flux could be easily doubled. It was also shown in this study that the flux enhancement was maximal when particle deposit was more severe (high feed concentration, low liquid flowrate) indicating that the mechanism responsible for this

enhancement is the disruption of the fouling layer. This was likely to arise from wall shear stress enhancement and pressure variations, which acted on the erosion/destabilisation of the deposit, thereby heightening the return mass flux of yeast cells and colloids towards the bulk suspension.

Z.F.Cui, et al. (2003) investigated performance and mechanism of flux enhancement with gas sparging in downwards crossflow ultrafiltration. They reported the results for gas-liquid two-phase co-current downwards crossflow ultrafiltration using a commercially available tubular membrane module. The performance of this operation was compared to that with co-current upwards crossflow operation. In this experiment, the membrane module was installed vertically where the feed solution and the injected gas bubbles flow downwards inside the membrane tubes. The parameters studied in this work included liquid and gas flow rates, TMP and feed concentration. Overall, it was observed that gas sparging can enhance ultrafiltration in the downwards crossflow operation. The permeate flux was improved by a maximum of 320%. The gas addition process led to significant enhancements in flux for both upwards and downwards flow. The enhancement was not affected by the time when the gas was injected to the stream, either at start or later on during the filtration. This is a clear indication on that gas sparging is effective both to prevent the formation of concentration polarisation layer and to disrupt the formed concentration.

In this experiment, where the feed consisted of dextrane solution and the concentration polarisation layer, dextran was the main reason for flux decline. The formation of the concentration polarisation layer in this case was reversible. The situation would be different if membrane fouling is significant. For example, to enhance microfiltration of yeast solution, where pore blocking and cake formation are expected to be the main mechanisms for flux decline, gas must be injected at the very beginning of the operation, and gas sparging fails to recover the flux after the membrane got fouled.

As for the effect of TMP and solution concentration, the trends followed similar trends as of conventional operation in which the highest amount of permeate flux is achieved at the highest TMP and lowest feed concentration. It was shown that gas sparging can achieve higher enhancement where concentration polarisation is expected to be severe, that is, at high TMP and

high feed concentrations. Again, this is another clear indication that the mechanism of this enhancement is due to the suppression of concentration polarisation layer.

Furthermore, it was indicated that low flowrate gas sparging is most effective to enhance ultrafiltration in the liquid laminar flow region. Injecting bubbles is thought to promote early transition from laminar to turbulent flow (Cui, et al., 2003).

In a study Li, et al. (1998) used gas sparging technique on a flat sheet membrane to enhance the permeate flux. Two different membranes, polysulphone (PS) and polyethersulfone (PES), with a molecular weight cut-off of 100 kD, were used in the experiments. Four types of proteins, human serum albumin (HSA, 69 kDa), human immunoglobulin G (IgG, 160 kDa), bovine serum albumin (BSA, 67 kDa) and lysozyme (Lys, 14 kDa), were chosen as the test media. The effects of gas sparging on permeate flux at different gas flowrates were investigated. Overall, the gas sparging was proven to be effective in increasing the permeate flux. Figure 4 shows the permeate flux for IgG and HSA with PES membranes at different air flowrates. It can be seen from this figure that the enhancement in permeate flux is not sensitive to the increase of air flow rate beyondbeyond 100 mL/min.

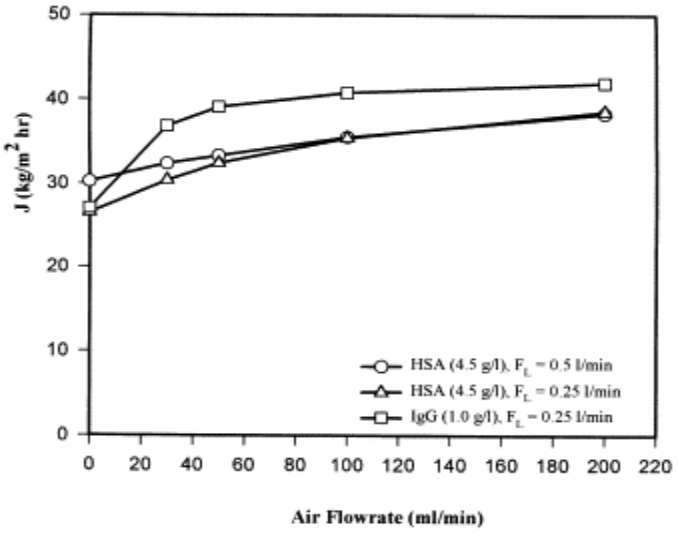

Figure 4- Effect of air flow rate on permeate flux in the ultrafiltration of single protein solutions (flat sheet module, PES membrane, TMP=0.3 bar, 20 mM phosphate buffer, pH 8.0) (Li, et al., 1998).

The results are in accordance with the previous findings by the same authors in tubular and hollow fibre membrane modules. Also, the gas sparging is found to be more effective for the operation in lower liquid flow rates where the degree of concentration polarization is higher.

The enhancement of permeate flux by gas sparging is through induction of secondary air bubble flow. The secondary flow around the air bubbles promotes the local mixing and reduces the thickness of mass transfer boundary layer which consequently results in increased mass transfer coefficient. As a result, the mass transfer rate of solute molecules from the membrane surface back to the bulk solution is increased, and the wall concentration is reduced. Therefore, it is expected that gas sparging will be more effective in a system where flux decline is dominated by concentration polarisation than a system with both concentration polarisation and deposit attachment as fouling mechanism. In the systems where deposit attachment is main mechanism of fouling, flux enhancement by gas sparging is much less effective than in those without deposit attachment and pore blocking (Li, et al., 1998).

Fouladitajara, et al. (2014) studied the effect of different two-phase flow patterns on permeate flux improvement and fouling resistance in a flat sheet membrane module. In this study, microfiltration of whey was performed through gas sparging as the method of fouling reduction under various air and liquid flow velocities corresponding to different flow patterns. A 0.45 µm pore size flat sheet polyvinylidene fluoride (PVDF) membrane (Millipore, USA), with 70% porosity and hydrophilicity behavior was used for all the experiments and the feed was prepared by magnetically stirring 500 g of whey powder, supplied by Kalleh Dairy Co., Iran.

The gas–liquid two-phase flow patterns were observed during the experiments which allowed for the explanation of permeate enhancement. Gas introduction at low flow rates produced a sparse bubbly flow which had no effect on the permeate flux for high liquid velocities; however, permeate flux was enhanced at higher proportions of injected gas. It was concluded that in turbulent liquid flow stream, induced small bubbles could not enhance the flow regime, and consequently the wall shear stress. (Fouladitajara, et al., 2014)

More flux enhancement was obtained in the case of lower liquid flow rates where particle deposit and concentration polarization effect were more severe. It is noteworthy that for a given liquid flow rate, the presence of bubbles and/or gas slugs increases the mean fluid velocity which, in association with the great variations in the wall shear stress and the existing turbulence in the wake of the bubbles, can enhance the membrane efficiency.

It was also found that the main mechanism responsible for this enhancement is the disruption of the fouling layer. This was rechecked by resistance in series of analyses in which the reversible fouling resistance showed to be the dominant one in various operating conditions. According to the analysis by the shear stress number and the resistance number, gas sparging found to be efficient to enhance permeate flux in most of the operating conditions, but it failed to remove deposit attachment and pore blocking, even with increasing proportions of injected gas. Shear stress number (N_s') and the resistance number (N_f) are defined as following for gas sparged systems (Fouladitajara, et al., 2014).

$$N_f = {\rho_L u_L^2}/{TMP} \qquad (1)$$

$$N_s' = {\rho'(u_g + u_L)^2}/{TMP} \qquad (2)$$

1.3 Gas Back Pulsing

Gas back pulsing can be considered the combination of two techniques of backwashing and air sparging for fouling removal. Gas back pulsing consists of gas being sequentially flushed backward through the membrane and passing through the pores. This method improves the filtration process through mechanisms mostly similar to regular backwashing. First, the concentration of the foulants or concentration polarization is disturbed near the membrane surface. Secondly, the pores are flushed inside out, and the particle deposits are detached from membrane surface, which can then be carried away by concentrate flow in crossflow filtration. Due to use of gas instead of permeate in gas back pulsing there is no loss of permeate in this technique. However, the forward filtration and permeate production is paused during gas back pulsing. Despite having been proven effective in enhancing permeate flux, there are relatively few studies on gas back pulsing. The common gas in use in this approach is air, as in air sparging, however, the effect of nitrogen and ozone gases have also been investigated by Park, et al. (2007) and Kim, et al. (2007). These studies will be further discussed in the following.

Chemical stability of the membrane is a matter of question when gases other than air are employed. Polymeric membranes are more sensitive to chemical agents, while membranes that

are made of ceramic materials (e.g., alumina, zirconia, and titanium) can sustain chemically enhanced gas back pulsing. (Fujioka, et al., 2015)

Air back pulsing was performed by C.Visvanathan, et al. (1997) on a 0.1 µm hollow fiber membrane module immersed in an activated sludge aeration tank. This study investigated 1) the possibility of membrane module for effluent filtration and air diffusion alternately in a cycle, 2) the effect of operation cycle (effluent filtration and air diffusion) in membrane bioreactor to prolong its operational life, and 3) operational stability parameters for membrane bioreactor. The effect of alternative air diffusion and effluent filtration on short term performance of the hollow fiber membrane was investigated under a batch operation for the duration of 8 hours. The following six different modes were studied: (1) continuous operation (2) 60:60 (3) 30:30 (4) 15:15 (5) 10:10 (6) 5:5 where 60:60 means 60 minutes of filtration and 60 minutes of air back pulsing. After each run the membrane was cleaned by soaking it in 2.5% sodium hypochlorite solution for 30 minutes.

Results show that continuous operation experienced a rapid decrease in flux with time, while the cyclic operation (discontinuous mode) could partially recover the flux after air back pulsing. Although cyclic operation couldn't completely remove the clogging which was observed by gradual decrease of permeate flux by time, air back flush technique was able to improve the flux by 371% compared to continuous operation. Also, permeate net cumulative volume was increased. The permeate flux improvement was attributed to two factors: removal of external deposit on membrane surface, thus preventing the compaction of cake layer under filtration pressure and removal of the particles which clog the membrane pores.

Overall, this study proved that the membrane air diffusion/back pulsing process plays a significant role in the improvement of permeate flux. By considering recovery of permeate flux and net cumulative permeate volume 15:15 (15 minutes of filtration followed by 15 minutes of air diffusion) cycle was found to be the optimum operation mode.

Park, et al. (2007) investigated the effect of N_2-back-flushing in multichannels ceramic microfiltration system for wastewater treatment of a toilet paper manufacturing plant. The membranes used in this research were 7 channels ceramic membrane HC10 (average pore size: 1.0 µm) and HC04 (0.4µm) and the wastewater source was the wastewater discharged from a

company making toilet papers by recycling milk or juice cartons. To see the effect of N2-back pulsing, back pulsing time (BT) was fixed at 40 s and filtration time (FT) was varied as 4, 8, 16 and 32 min. The N2-back-flushing pressure was fixed at 5.0 kgf/cm2, TMP at 1.0 kgf/cm2 (98.06 Kpa) and the feed flow rate at 2.0 L/min. The effect of N2 filtration time on membrane fouling resistance was measured using resistance in series equation. The resistance-in-series filtration equation is known well in the application field of membrane separation and is as follows:

$$J = \Delta P/(Rm + Rb + Rf) \qquad (3)$$

where J is the permeate flux through membrane, ΔP is TMP (trans-membrane pressure), R_m the resistance of membrane, R_b the resistance of boundary layer, and R_f the resistance of membrane fouling. For filtration of pure water, R_b and R_f do not exist because of no boundary layer by concentration polarization and no membrane fouling by pollutants. Eq (3) could be simplified to Eq (4).

$$J = \frac{\Delta P}{Rm} \qquad (4)$$

Now R_m could be calculated from the experimental data of permeate flux for pure water using Eq (4). Then, the plot of $R_b + R_f$ vs. t (operation time) could be obtained from the permeate flux data using wastewater. The intercepting value of y-axis ($t = 0$) in this plot using only initial two or three data is R_b because of no R_f at the initial time of filtration, and finally R_f could be calculated using Eq (3).

In conclusion, the N2 back pulsing proved to be an effective method to improve the permeability of both HC10 and HC04 membranes comparing to the condition where no back pulsing was performed in this system.

for HC10 (pore size 1.0 µm), FT = 16 min was found to be the most effective filtration time at BT = 40 s to reduce membrane fouling and to maintain high permeate flux during filtration in this system; confirmed by highest amount of highest total permeate at this filtration time. For HC04 (pore size 0.4 µm) membrane the lowest value of Rf was obtained at FT = 4 min and BT = 40 s. The optimal FT of 4 min for HC04 was much lower than the optimal FT of 16 min for HC10 membrane, which means that HC04 with smaller pore size than that of HC10 needs more frequent N2-back-flushing to reduce membrane fouling and to maintain high flux.

It is reported that intermittent ozonation is effective in preventing membrane fouling caused by particle accumulation. Intermittent ozone back washing was investigated by Kima, et al. (2007) as a method for membrane fouling reduction in a submerged metal membrane. The purpose of this research was to investigate the effect of ozone backwashing for permeation flux recovery. In order to investigate the effect of ozone back washing in this work, six separate experimental runs were conducted for flux recovery, using air or ozone gas backwashing and fresh or synthetic sewage as the feed.

The permeation flux variations as a function of time with air back washing or ozone back washing is shown in Figure 5 for the six runs.

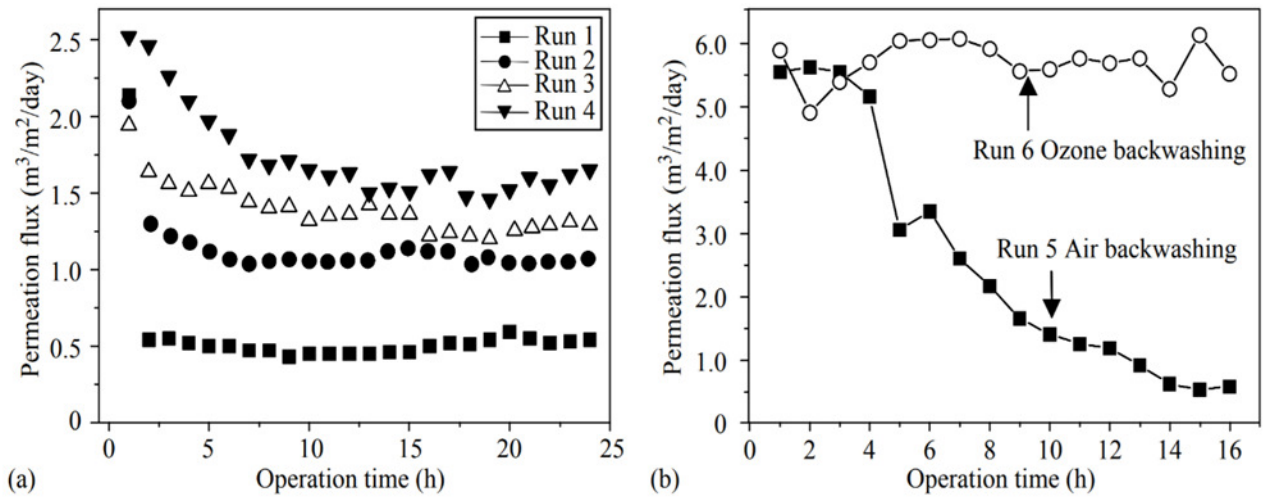

Figure 5- Flux variations as a function of time in the case of air backwashing and ozone backwashing. [Conditions: (a) feed: fresh sewage (b) feed: synthetic sewage, pore size 1 (mm), pressure: 50 (kPa)]. (Kim, et al., 2007

It can be seen from the results that the ozone backwashing could effectively recover the permeation flux in microfiltration system and prolong the period to reach the steady state flux rather that air back washing. Regarding the operational parameters, the increase of ozone gas flowrate (Run 4) for the recovery of permeation flux was more effective than the prolongation of the injection time (Run 3) under the same ozone doses.

Figure 6 presents the variation of permeation flux and flux ratio (J/J0) as a function of operational time, the results suggests that intermittent ozone backwashing was more effective than the air back washing in fouling removal. In case of air backwashing, flux recovery ratio was about 80%, while it showed over 90% of recovery when ozone backwashing was applied.

As the filtration/backwashing cycle was longer, the effect of flux recovery by ozone backwashing decreased. Therefore, it is favorable to operate membrane cleaning before the foulant is consolidated on the membrane surface.

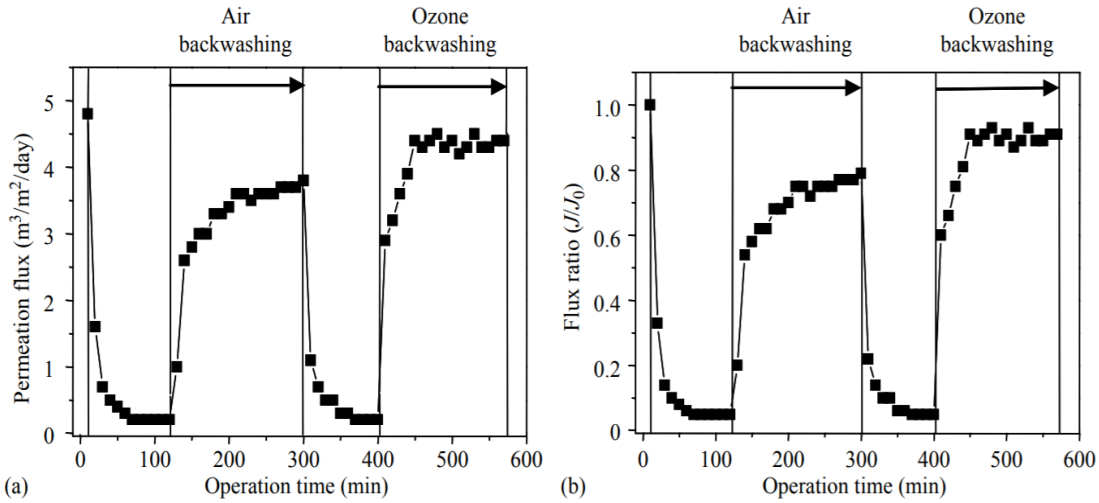

Figure 6-The variation of flux and J/J0 in the case of air backwashing and ozone backwashing with fresh sewage. [Conditions: gas flow rate 6 (L/min), ozone concentration 58 (g/m3), backwashing time 2 (min), filtration time 30 (min), pore size 1 (mm)]. (Kim, et al., 2007)

The applicability of periodic air-backwash to alleviate crystal fouling in submerged VMDC for inland brine water treatment was investigated in a study by Julian, et al. (2018). Using polypropylene membrane and modelled inland brine solution at very high concentrations, the effect of air-backwash was evaluated against water production for operation parameters: air backwash pressure, frequency and duration. As periodic air-backwash introduced air bubble to the feed solution which can promote heterogeneous nucleation and increase the CaCO3 crystal yield in the feed solution, excessive air-backwash (frequency and duration) resulted on deposition of Mg on the membrane which led to denser fouling layer. Optimization of periodic air-backwash pressure (200 kPa), frequency (in every 60 min) and duration (30 s) in this particular study resulted on 150% permeate productivity improvement from 79 L m−2 for the test without air-backwash to 196 L m−2 for the test with air-backwash at optimized condition (Julian, et al., 2018).

Chapter Two: Materials and Methods

Current experimental study aims to investigate the effect of air back pulsing on fouling control in microfiltration of dairy wastewater. The parameters under study are air pressure, back pulsing frequency and back pulsing duration. In this chapter, the experimental method and the materials used are explained in detail.

2.1 Model dairy wastewater

A model dairy wastewater was used as the feed in this experiment. The feed was prepared using skim milk diluted with distilled water (milk:water = 1:2) to one third of normal concentration. The skim milk was prepared using skim milk powder (No Name skim milk powder, Loblaws Canada). According to the milk powder package, 100 grams of powder plus a liter of water would give a liter of skim milk. Therefore, for the 20-liter feed tank to be filled, 6.6 liters of skim milk was prepared and topped up with 13.4 liters of distilled water to give 1:2 dilution. For the experiments corresponding to Response Surface Methodology design, 2 liters of skim milk was topped up with 18 liters of distilled water to give 1:9 dilution. According to the previous studies, the effluent compositions and filtration behaviors for this model dairy effluent and the real dairy wastewater are very similar. (Zhanga, et al., 2017)

2.2 Membrane type

As for the membrane, the Synder flat sheet PVDF membrane, V01 available at Sterlitech Corporation (SKU: YMJXSP3001) was used. The specifications of the membrane are presented in Table 1.

Table 1-membrane specifications

Series	Synder V01
Feed	Industrial/Dairy
Type	"Intermediate", Fat/Microbial Removal, Protein Fractionation
PH range (25 °C)	1-11
Flux (GFD)/PSI	237-254/20

Pore size/MWCO	0.1 µm
Polymer	PVDF
Sheet size	(305×305) mm^2
Membrane thickness	0.2 mm
Filtration active area	(18.3 *10.15) cm^2

2.3 Experimental setup

A flat sheet membrane module was specially designed and fabricated for this study, Figure 7. The module was made up of two thick acrylic (polymethylmethacrylate) stacked plates. The dimension of flat sheet module was 25.4 cm in length and 12.5 cm in width. The filtration surface was 18.3 cm long and 10.15 cm wide providing a total active area of 185.8 $cm^2\mathrm{cm}^2$. Two O-rings were placed between the two acrylic plates to ensure that the module was completely sealed.

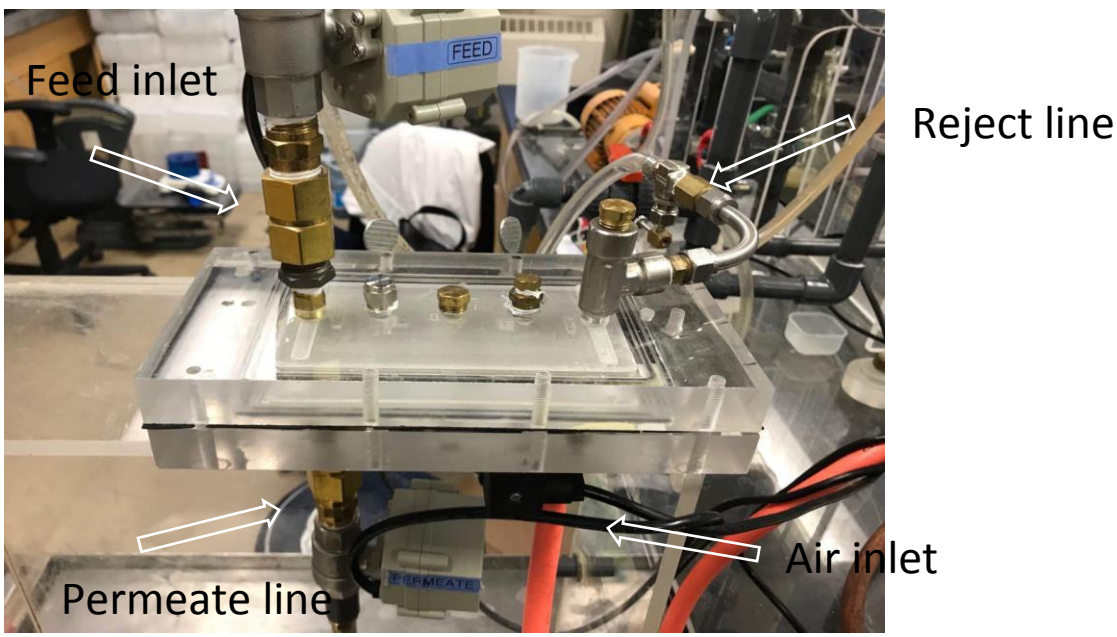

Figure 7-The flat sheet filtration module.

As it can be seen in the schematic diagram of the experimental set up, Figure 8, the feed is pumped toward the membrane setup using a centrifugal pump. The feed is prepared in a 20-liter tank. As the cross-flow filtration takes place, the feed sequentially flows across the membrane surface, resulting in the concentrate stream and the permeate stream. The concentrate stream

(reject liquid) leaves the setup from the top and the permeate stream (filtered liquid) leaves from the bottom.

Air is supplied from a compressed air line in the laboratory. The pressure of the air is controlled via an air regulator. The back pulsing is performed by air, flowing sequentially upwards from the lower plate (permeate compartment), passing through the membrane and exiting the membrane module through the reject line.

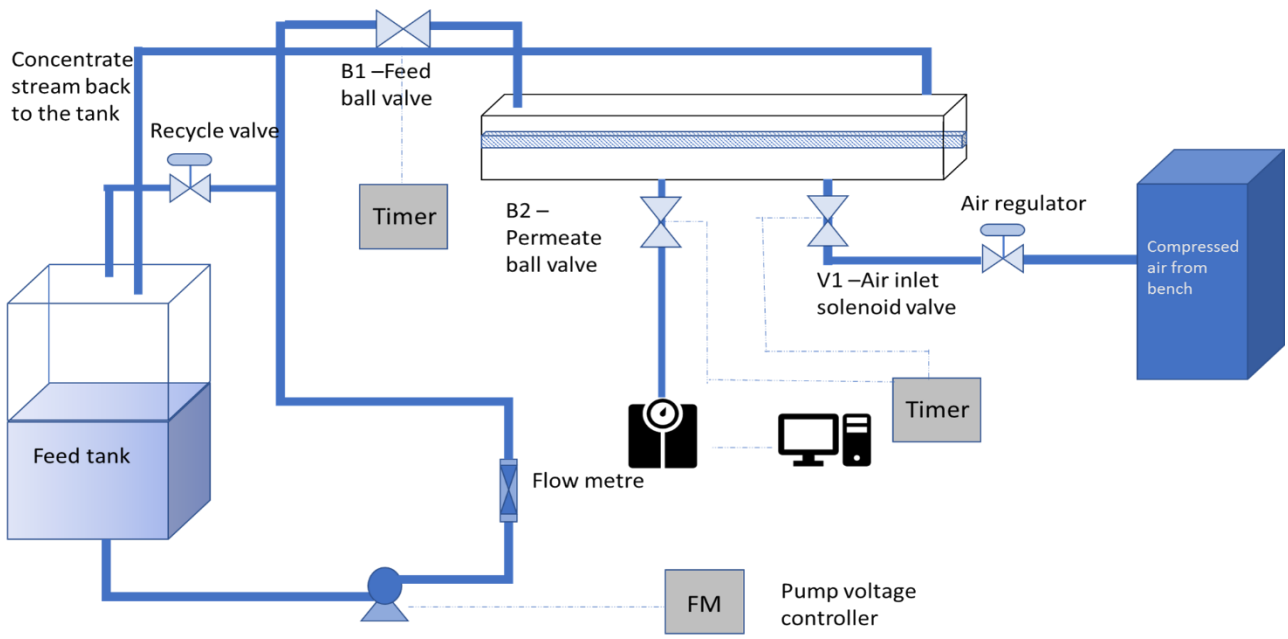

Figure 8-Schematic presentation of the experimental setup

In order to open and close the feed, permeate and air valves sequentially, two ball valves and a solenoid valve, respectively, were employed on the stream lines. The valves were commanded open/close by two programmable timing controllers. The specifications of the equipment used in the setup is presented in Table 2.

Table 2- Equipment specifications

Equipment	Specification
Centrifugal pump	Halm motors, Type: WB71B2, 220 Volts
Balance	OHAUS Adventure pro Balance, Model number: AV2101C
Air pressure regulator	Mastercraft air pressure regulator, SCFM flow: 26 @90 PSI, provides regulated output pressure between: 0-125 PSI
Ball valves	
Digital timers	

The permeate was collected in a container placed on a digital balance, connected to a computer through a hyper terminal connection. The permeate weight was recorded every 5 seconds during each run.

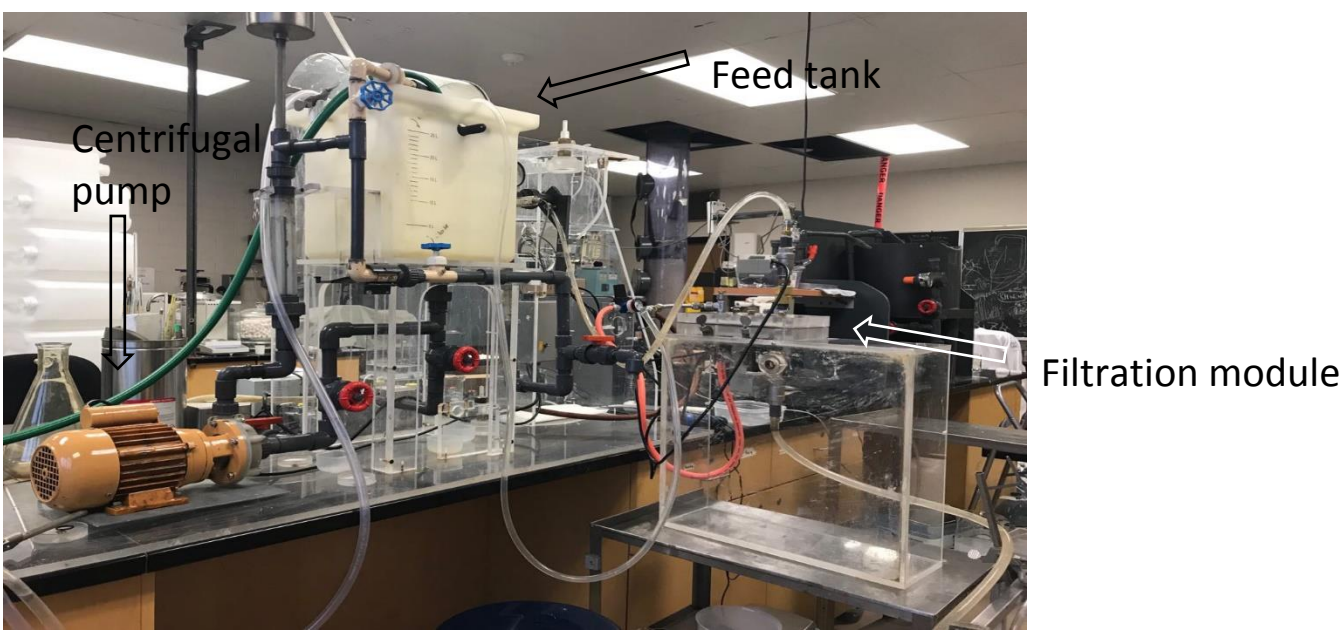

Figure 9-Experimental setup

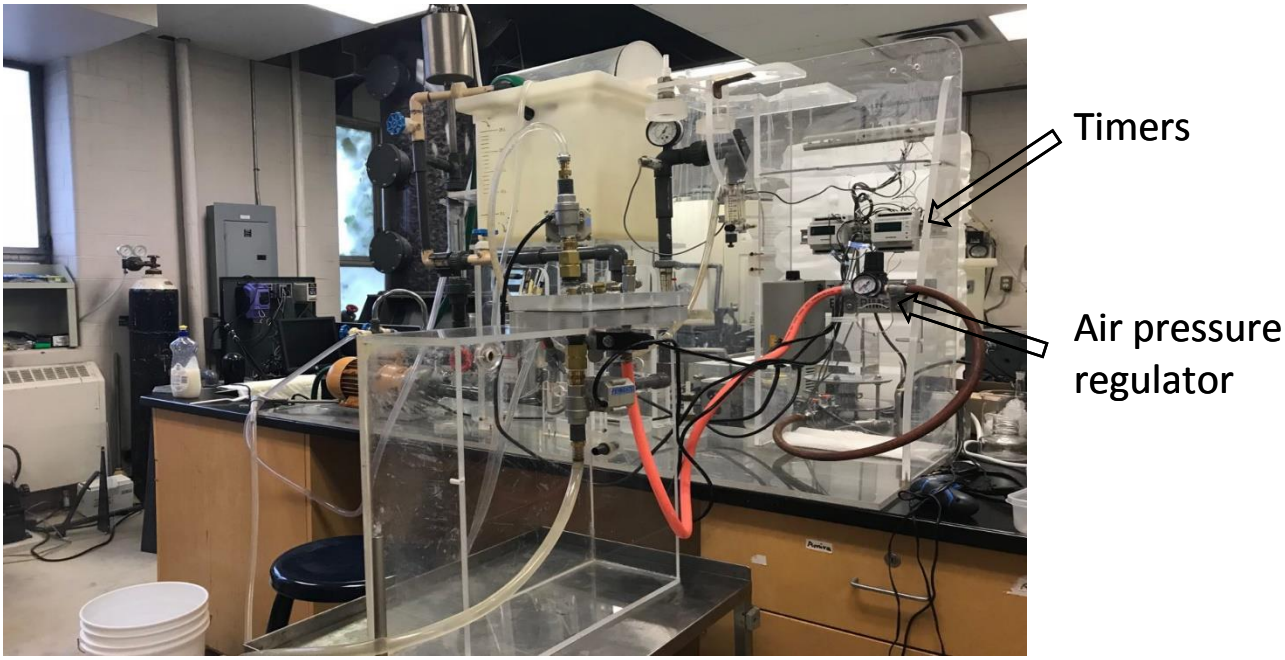

Figure 10-Experimental setup

2.4 Design of Experiments

One strategy of experimentation that is used extensively in practice is the one factor-at-a-time (OFAT) approach. The OFAT method consists of selecting a starting point, or baseline set of levels, for each factor, and then successively varying each factor over its range with the other factors held constant at the baseline level. After all tests are performed, a series of graphs are usually constructed showing how the response variable is affected by varying each parameter with all other factors held constant.

The major disadvantage of the OFAT strategy is that it fails to consider any possible interaction between the factors. An interaction is the failure of one factor to produce the same effect on the response at various levels of another factor. One factor-at-a-time experiments are always more costly and less efficient than other methods based on a statistical approach to design.

The correct approach to dealing with several factors is to conduct a factorial experiment. This is an experimental strategy in which factors are varied together, instead of one at a time and

are most efficient form in experiments which involve the study of the effects of two or more factors.

In a factorial design, each complete trial or replicate of the experiment, all possible combinations of the levels of the factors are investigated. For example, if there are “a” levels of factor A and “b” levels of factor B, each replicate contains all “ab” treatment combinations. When factors are arranged in a factorial design, they are often said to be crossed.

The effect of a factor is defined to be the change in response produced by a change in the level of the factor. This is frequently called a main effect because it refers to the primary factors of interest in the experiment.

2.4.1 The 2^k factorial design

The most important of factorial designs is that of k factors, each at only two levels. These levels may be quantitative, such as two values of temperature, pressure, or time; or they may be qualitative, such as two machines, two operators, the “high” and “low” levels of a factor, or perhaps the presence and absence of a factor. A complete replicate of such a design requires $2 \times 2 \times \ldots \times 2 = 2^k$observations and is called a 2k factorial design.

Generally, if there are k factors, each at two levels, the factorial design would require 2^k runs. Clearly, as the number of factors of interest increase, the number of runs required increases rapidly; for instance, a 10-factor experiment with all factors at two levels would require 1024 runs. This quickly becomes infeasible from a time and resource viewpoint.

If there are four to five or more factors, it is usually unnecessary to run all possible combinations of factor levels. A fractional factorial experiment is a variation of the basic factorial design in which only a subset of the runs is used.

The 2^k design is particularly useful in the initial stages of experimental work when many factors are likely to be investigated. It provides the smallest number of runs with which k factors can be studied in a complete factorial design. Consequently, these designs are widely used in factor screening experiments.

Because there are only two levels for each factor, it is assumed that the response is approximately linear over the range of the factor levels chosen. In many factor screening

experiments, when starting to study the process or the system, this is often a reasonable assumption.

2.5 Response Surface Methodology

Response surface methodology, or RSM, is a collection of mathematical and statistical techniques useful for the modeling and analysis of problems in which a response of interest is influenced by several variables and the objective is to optimize this response. An example is a response variable y as function of x_1 and x_2.

$y = f(x_{1,}x_2) + \varepsilon$ Eq (5)

Where ε represents the noise or error observed in the response y. Response surface is usually represented graphically, such as in Figure 11, where y is plotted versus the levels of x_1 and x_2.

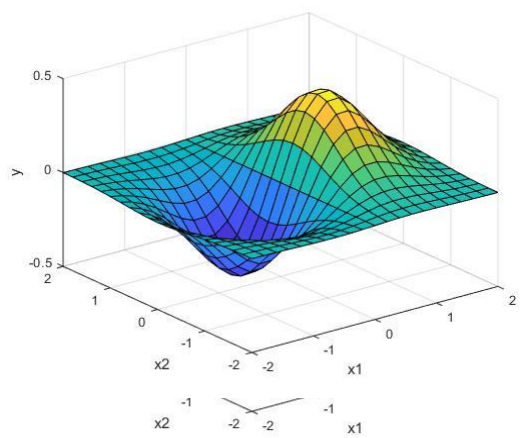

Figure 11- A three-dimensional response surface as a function of ($x_{1,}$) and (x_2)

In most RSM problems, the form of the relationship between the response and the independent variables is unknown. Thus, the first step in RSM is to find a suitable approximation for the true functional relationship between response variable and the set of independent variables. Usually, a low-order polynomial in some region of the independent variables is employed. If the response is well modeled by a linear function of the independent variables, then the approximating function is the first-order model.

$y = \beta_0 + \beta_1 x_1 + \beta_2 x_2 + \beta_3 x_3 \dots\dots. + \beta_k x_k + \epsilon$ Eq (6)

If there is curvature in the system, then a polynomial of higher degree must be used, such as the second-order model.

$$y = \beta_0 + \sum_{i=1}^{k} \beta_i x_i + \sum_{i=1}^{k} \beta_{ii} {x_i}^2 + \sum\sum_{i<j} \beta_{ij} x_i x_j + \epsilon \qquad \text{Eq (7)}$$

Almost all RSM problems use one or both models. Of course, it is unlikely that a polynomial model will be a reasonable approximation of the true functional relationship over the entire space of the independent variables, but for a relatively small region they usually work quite well (Montgomery, et al., 2003).

The method of least squares is used to estimate the parameters in the approximating polynomials. The response surface analysis is then performed using the fitted surface. If the fitted surface is an adequate approximation of the true response function, then analysis of the fitted surface will be approximately equivalent to analysis of the actual system. The model parameters can be estimated most effectively if proper experimental designs are used to collect the data. Designs for fitting response surfaces are called response surface designs. In this research case, Central Composite Design is used for the RSM study. RSM is a sequential procedure. Often, when a point on the response surface is remote from the optimum, such as the current operating conditions, there is little curvature in the system and the first-order model will be appropriate. The objective is to lead the experimenter rapidly and efficiently along a path of improvement toward the general vicinity of the optimum. Once the region of the optimum has been found, a more elaborate model, such as the second-order model, may be employed, and an analysis may be performed to locate the optimum. The analysis of a response surface can be thought of as "climbing a hill," where the top of the hill represents the point of maximum response. If the true optimum is a point of minimum response, then we may think of "descending into a valley".Figure 12.

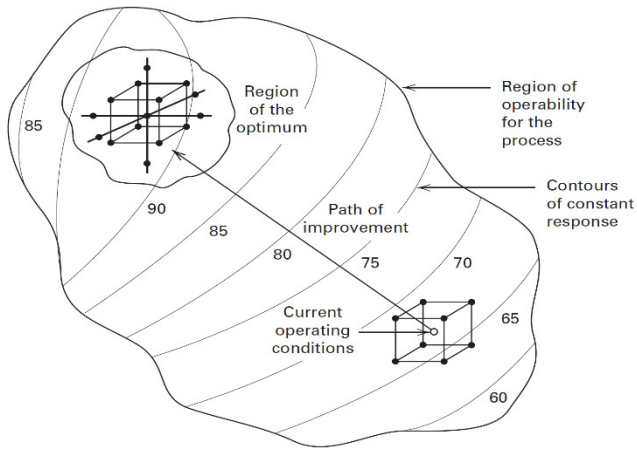

Figure 12-The sequential nature of RSM

The eventual objective of RSM is to determine the optimum operating conditions for the system or to determine a region of the factor space in which operating requirements are satisfied.

2.6 Experimental procedure

2.6.1 Filtration test

A 0.1 µm pore size polyvinylidene fluoride (PVDF) membrane was placed in the membrane module for each run. After each run, the membrane was left to be air dried and kept for the further solid content measurements and Scanning Electron Microscope (SEM) Imaging. The filtration took place at trans-membrane pressure (TMP) of 28 psi, feed flowrate of 2 Liter per minute (LMP) and total run time of 10 minutes.

During each run the feed, permeate and air valves opened and closed sequentially according to scheme 1.

Table 3-Scheme 1

Feed Valve	Open	Close
Permeate valve	Open	Close
Air valve	Close	open

In order to obtain a reasonable range for the parameters under study, a filtration run was performed using the model wastewater until a steady permeate flux was reached. Based on overall filtration time to reach steady permeate flux the levels of back pulsing frequency and duration were proposed. In the first stage, the filtration was run for overall of ten minutes, and

the levels of two parameters (factors) were held constant while the level of the third parameter was changed. During the first step, the level of pressure was changed at 10, 15, 20, 25 and 30 psig while the back pulsing duration and frequency were maintained at 30 seconds. The optimum pressure from this step was then determined and used in the second step where the pressure and frequency levels were fixed and back pulsing duration varied at 30, 45, 60 and 75 seconds. Again, the optimum back pulsing duration from this step was determined and used in the last step where the pressure and duration levels were fixed at the optimum levels from previous steps. The back pulsing frequency (time elapse between two consecutive back pulsing cycles) levels varied at 30, 45, 60 and 75 seconds. Finally, the optimum levels for the three parameters were determined as the ones that yielded the highest amount of permeate. The data from this stage is presented in Appendix A.

At the next stage, the Response Surface Methodology analysis was performed using Design-Expert® Software Version 11 for further investigation of the system and finding the actual optimum point in the design space. The preliminary optimum found in the previous stage was fed to the software as a starting point. The Central Composite Design, Table 4, was provided by the software for RSM analysis. The design consists of a total of 20 runs that are randomly spread through three blocks of Day 1, Day 2 and Day 3. Blocking is a technique for dealing with unexplained variability or random error.

Table 4-RSM design

				Factor 1	Factor 2	Factor 3	Response 1
Std	Block	Run	Space Type	P: Pressure	D: Duration	F: Frequency	permeate amount
				psi	s	s	
7	Day 1	1	Factorial	15	60	90	
1	Day 1	2	Factorial	15	30	60	
10	Day 1	3	Center	20	45	75	
4	Day 1	4	Factorial	25	60	60	
9	Day 1	5	Center	20	45	75	
6	Day 1	6	Factorial	25	30	90	
5	Day 2	7	Factorial	15	30	90	

3	Day 2	8	Factorial	15	60	60	
2	Day 2	9	Factorial	25	30	60	
11	Day 2	10	Center	20	45	75	
12	Day 2	11	Center	20	45	75	
8	Day 2	12	Factorial	25	60	90	
17	Day 3	13	Axial	20	45	49.7731	
13	Day 3	14	Axial	11.591	45	75	
20	Day 3	15	Center	20	45	75	
15	Day 3	16	Axial	20	19.7731	75	
14	Day 3	17	Axial	28.409	45	75	
16	Day 3	18	Axial	20	70.2269	75	
18	Day 3	19	Axial	20	45	100.227	
19	Day 3	20	Center	20	45	75	

The experiment was conducted by changing the levels of parameters according to the design shown above. The data collected is presented in Appendix A.

2.6.2 Scanning Electron Microscope Imaging.

A scanning electron microscope (SEM) is a type of electron microscope that produces images of a sample by scanning the surface with a focused beam of electrons. The electrons interact with atoms in the sample, producing various signals that contain information about the surface topography and composition of the sample. In membrane technology, SEM imaging is extensively used to obtain information about membrane surface properties characteristics such as such as pore size, pore size distribution, pore shape, porosity, surface roughness, fouling, etc (Z.Abdullah, et al., 2014).

In this work SEM imaging is used to observe and qualitatively analyze fouling on different membrane samples and to compare the effect of back pulsing on fouling mitigation.

Chapter Three: Results and Discussion

In this chapter, analysis of the raw data obtained following the OFAT approach and Central Composite Design is presented and the corresponding results are discussed in detail.

3.1 Parameters' Level Investigation

In order to obtain a reasonable range for the parameters under study a filtration run was performed using the model wastewater until a steady permeate flux was reached. Based on overall filtration time to reach steady permeate flux, the levels of back pulsing frequency and duration were proposed and further investigated following an OFAT approach. The cumulative permeate amount versus time for the run with no back pulsing is shown in Figure 14. The permeate increased until around 220 seconds (3.6 minutes) sharply; after that the flux gradually declined and reached a plateau beyond 500 seconds. Therefore, total filtration time of ten minutes was chosen and the parameter levels were proposed accordingly in the following stage. Data for the experiments conducted without back pulsing are available in Appendix A, Table 11.

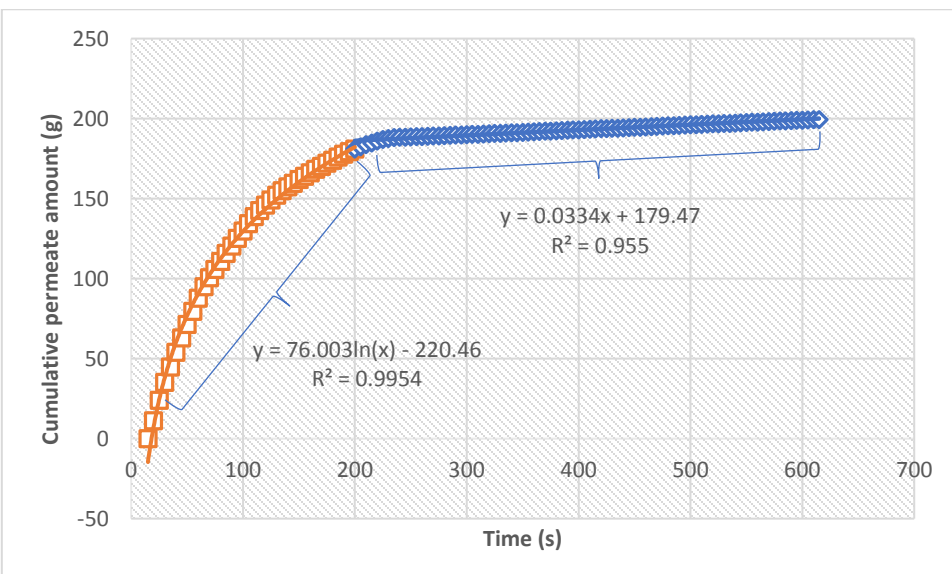

Figure 14- Cumulative permeate amount vs time in a run with model feed and no back pulsing, TMP=28 psi, Q=2 LMP

Following the OFAT approach, the level of one parameter was changed while keeping the levels of the other two parameters constant. Firstly, the level of pressure was set to 10, 15, 20,

25 and 30 psig. The back pulsing duration and frequency were both held constant at 30 seconds. The cumulative permeate amount vs pressure is shown in Figure 15. It can be seen that the highest amount of permeate was achieved at 20 psig; and therefore, 20 psig was chosen as the optimum pressure for testing of the next parameter (factor).

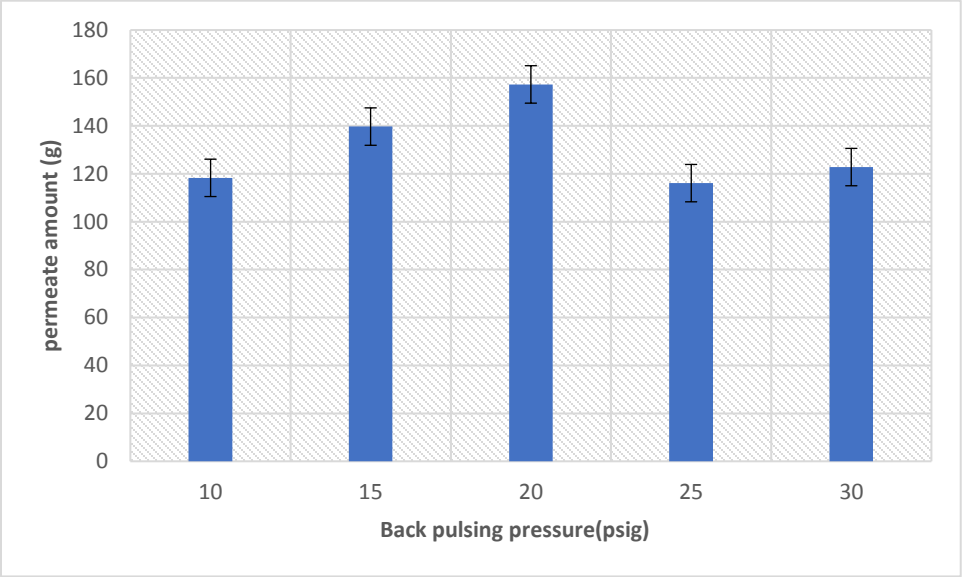

Figure 15-permeate amount vs back pulsing pressure (p_b), d=30s, f=30s

In the next step, the level of back pulsing frequency was set to 30, 45, 60 and 75s while keeping the pressure at 20 psig and frequency at 30s. Results obtained are presented in Figure 16. The maximum permeate amount in this step was achieved at 75 s. At the last step, the back pulsing duration was changed at 30, 45, 60 and 75 s while maintaining the pressure and frequency at 20 psi and 75 s, respectively. At this step, maximum amount of permeate was obtained at 45s of back pulsing duration.

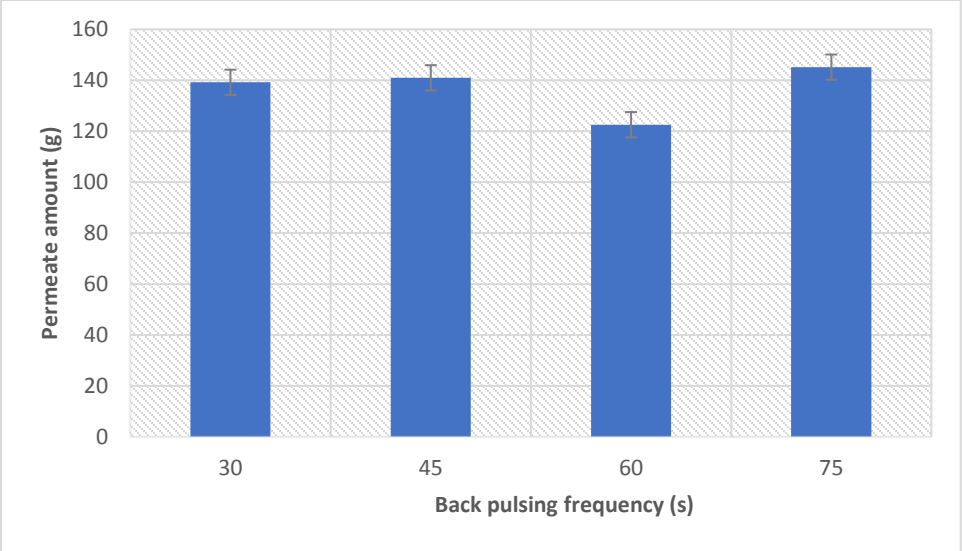

Figure 16-permeate amount vs back pulsing frequency (f), p_b=20 psig, d=30s

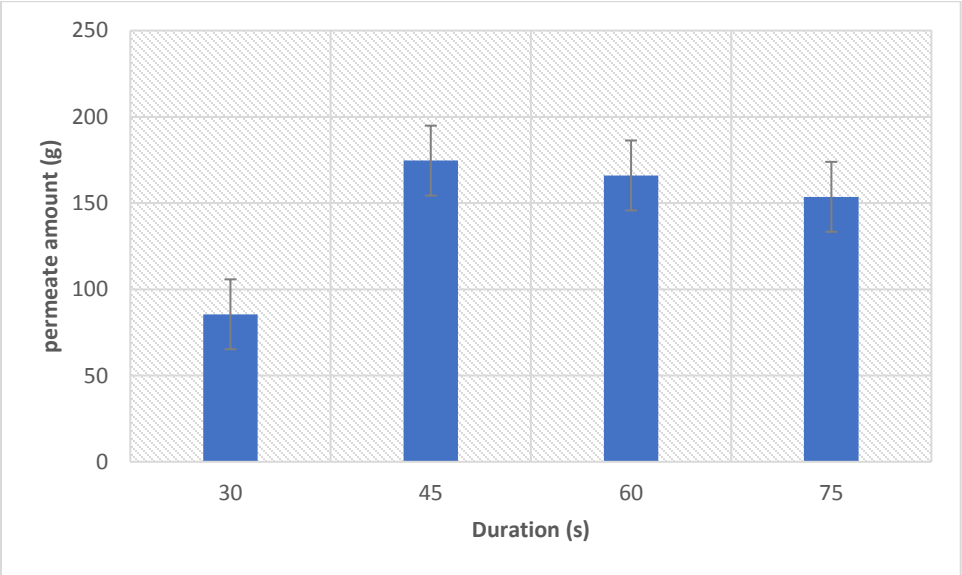

Figure 17-permeate amount vs back pulsing duration (d), p_b=20 psig, f=75s

Increasing back pulsing pressure improved the filtration process to a certain point, resulting in increased amount of permeate. However, at pressures beyond 20 psig permeate amount did not increase any further and in fact was decreased. It is anticipated higher pressures of back pulsing would improve the filtration process as it would create higher shear stress in the membrane pores and on the membrane surface. However, it is reported by previous studies that

higher air pressures could result in a change in nature of the fouling and in fact create a denser fouling layer (Julian, et al., 2018).

Back pulsing frequency is translated into filtration cycle. Therefore, higher frequencies mean longer filtration cycles; and hence, larger amount of permeate was obtained. However, if the filtration time is increased beyond a certain point the back pulsing duration would be too short and the back pulsing cycle would be too far apart to effectively mitigate fouling and improve the filtration process. In this case, filtration time of 75 seconds and back pulsing duration of 45 seconds gives the highest amount of permeate.

3.2 Response Surface Methodology Analysis of the Results

The RSM analysis of the data followed by the corresponding Central Composite Design and data collection is presented in this section. Firstly, the final value of accumulative permeate amount as the response variable was entered in the software. The results can be seen in the table below.

Table 5- RSM design table with the response variable values

				Factor 1	Factor 2	Factor 3	Response 1
Std	Block	Run	Space Type	P: Pressure	D: Duration	F: Frequency	permeate amount
				psi	s	s	gr
7	Day 1	1	Factorial	15	60	90	264.97
1	Day 1	2	Factorial	15	30	60	313.995
10	Day 1	3	Center	20	45	75	280.247
4	Day 1	4	Factorial	25	60	60	275.434
9	Day 1	5	Center	20	45	75	291.184
6	Day 1	6	Factorial	25	30	90	408.19
5	Day 2	7	Factorial	15	30	90	360.014
3	Day 2	8	Factorial	15	60	60	200.823
2	Day 2	9	Factorial	25	30	60	361.632
11	Day 2	10	Center	20	45	75	312.684
12	Day 2	11	Center	20	45	75	300.077

8	Day 2	12	Factorial	25	60	90	323.54
17	Day 3	13	Axial	20	45	49.7731	231.927
13	Day 3	14	Axial	11.591	45	75	273.469
20	Day 3	15	Center	20	45	75	291.618
15	Day 3	16	Axial	20	19.7731	75	377.312
14	Day 3	17	Axial	28.409	45	75	373.871
16	Day 3	18	Axial	20	70.2269	75	231.29
18	Day 3	19	Axial	20	45	100.227	365.041
19	Day 3	20	Center	20	45	75	296.086

3.2.1 Correlation Grid

The initial analysis is presented as a correlation grid. A correlation grid is a square grid displaying the correlation of different factors with each other and with the response variable. Each square in the correlation grid show the correlation of its row factor and column factor. Darker colors are indicative of higher correlation and lighter colors show low correlations of the factors. For example, the blue square in Figure 18 displays the correlation between permeate amount and duration and the correlation value is -0.708. The red along the diagonal indicates the complete (r=1) correlation of any variable with itself (Run vs Run, etc.). Block versus run (or, conversely, run vs block) is also highly correlated due to restriction in randomization (runs having to be done for day 1 before day 2).

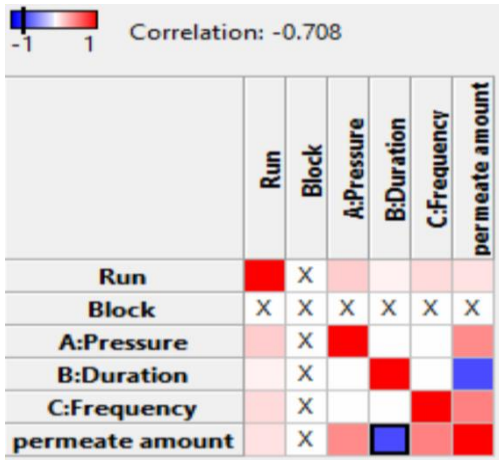

Figure 18-Correlation grid

It can be seen in the Figure 18 that the permeate amount has a high negative correlation with duration and positive correlation with pressure and frequency. Therefore, the amount of permeate will increase with an increase in pressure or frequency and will go down as the back pulsing duration go up. This result will be further discussed in the following sections.

3.2.2 Model Selection

The regression computation is carried out by the Design-Expert® Software to find a polynomial model best describing the experimental data. The method of least squares is used to estimate the regression coefficients in the approximating polynomial. The predictive model is presented in both actual and coded terms. The equation in terms of coded factors is as below:

$$permeate\ amount = +299.80 + 29.13 \times P - 45.74 \times D + 31.39 \times F + 10.36 \times P^2 \quad \text{Eq (8)}$$

The equation in terms of coded factors can be used to make predictions about the response for given levels of each factor. The high levels of the factors are coded as +1 and the low levels are coded as -1 per the formula below.

$$Coded: \frac{2\times(Actual\ setting - Average\ actual\ setting)}{Range\ between\ high\ and\ low\ actual\ setting} \qquad \text{Eq(9)}$$

For example, for the first observation in Table 5, the values of P, D and F are -1, +1 and +1, respectively. Plugging these values into equation (8) will give the corresponding permeate amount in the table. The coded equation is useful for identifying the relative impact of the factors by comparing the factor coefficients.

The equation in terms of actual factors is:

$$permeate\ amount = 329.26 - 10.74 \times P - 3.05 \times D + 2.09 \times F + 0.41 \times P^2 \quad \text{Eq}(10)$$

The equation in terms of actual factors can be used to make predictions about the response for given levels of each factor within their range of this study. Here, the levels should be specified in the original units for each factor. This equation should not be used to determine the relative impact of each factor because the coefficients are scaled to accommodate the units of each factor and the intercept is not at the center of the design space.

The predictive equations both have three linear terms, i.e. P, D and F and one quadric term, i.e. P^2. Therefore, the whole equation is of second order.

As suggested by the coded equation, the permeate amount is directly proportional to back pulsing pressure and frequency and inversely proportional to back pulsing duration. In other words, high pressures of air in short durations of back pulsing is more effective and will result in higher amounts of permeate. This is depicted by Figure 19 where relative effect of the factors is shown. However, it is anticipated that beyond the design space, very high frequency would not be helpful. Too high frequency (time elapse between two consecutive back pulsing cycles) means short back pulsing duration and this might result in loss of the positive effect of back pulsing as very short back pulsing durations would let for compaction of fouling cake layer under filtration pressure which is later difficult to be removed.

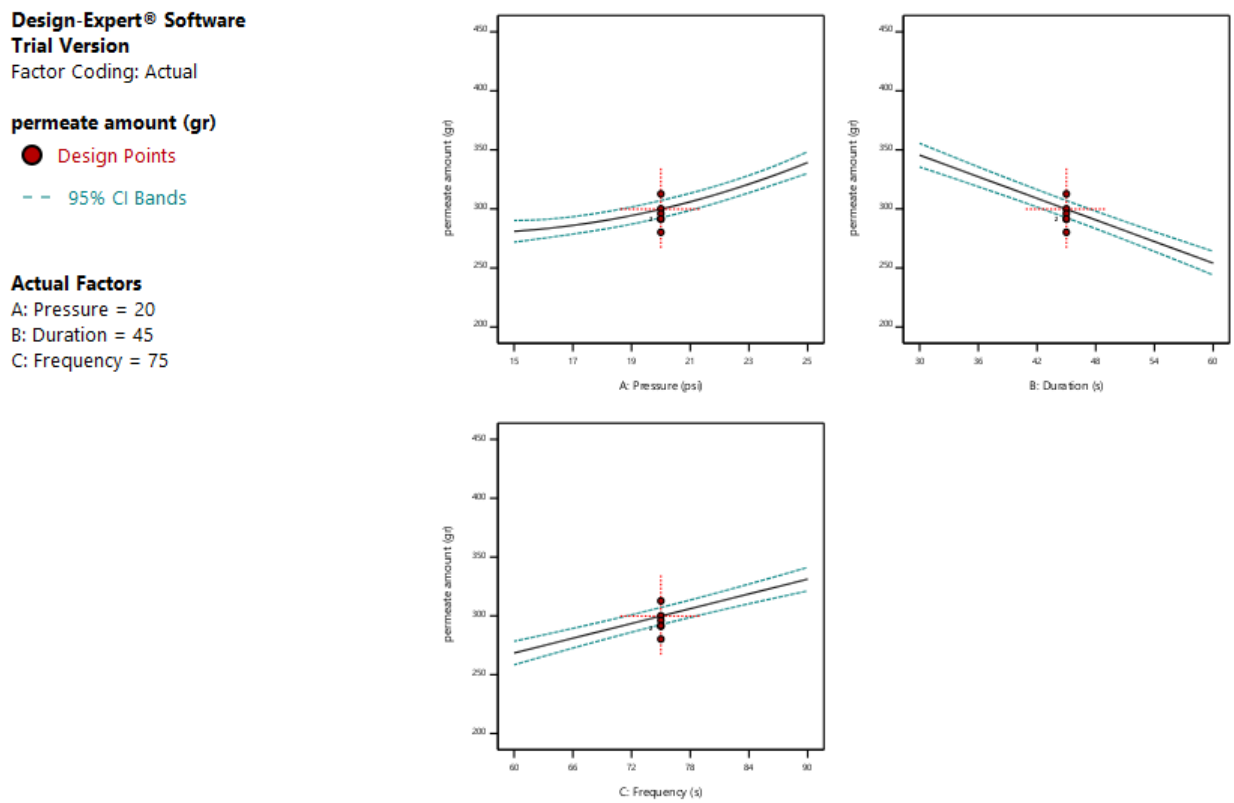

Figure 19- Relative effect of the factors

3.2.2.1 Analysis of Variance (ANOVA)

The Analysis of Variance is a method that is used to test for significance of regression. The procedure partitions the total variability in the response variable into two parts: systematic factors and random factors. The systematic factors have a statistical influence on the given data set, but the random factors do not. Analysis of Variance checks for significance of the systematic factors and the proposed model consisting of these factors. (Montgomery, et al., 2003). ANOVA for the current set of data checks for adequacy of the proposed quadric model through different statistical tests presented in *Table 6*. Here the response variable is the permeate amount and the statistical factors are back pulsing pressure, duration and frequency.

Table 6- ANOVA for Linear model of permeate amount

Source	Sum of Squares	df	Mean Square	F-value	p-value	
Block	84.89	2	42.45			
Model	55191.18	4	13797.79	100.00	< 0.0001	significant

A-Pressure	11590.12	1	11590.12	84.00	< 0.0001	significant
B-Duration	28570.23	1	28570.23	207.05	< 0.0001	significant
C-Frequency	13457.24	1	13457.24	97.53	< 0.0001	significant
A^2	1573.58	1	1573.58	11.40	0.0050	significant
Residual	1793.79	13	137.98			
Lack of Fit	1644.52	10	164.45	3.31	0.1770	not significant
Pure Error	149.27	3	49.76			
Cor Total	57069.86	19				

As shown in *Table 6*, the model F-value is 100.00, which implies the model is significant. There is only a 0.01% chance that an F-value this large could occur due to noise.

The P-value is the smallest level of significance that would lead to rejection of a model term in hypothesis tests. The choice of significance level at which the model terms are rejected is arbitrary. Conventionally authors refer to statistically significant as P is less than 0.05 and statistically not significant as P is greater than 0.10 (Montgomery, et al., 2003). Therefore, P-values less than 0.05 indicate model terms are significant and values greater than 0.10 indicate the model terms are not significant. In this case, $\mathrm{P}, \mathrm{D}, \mathrm{F}$ and P^2 are significant model terms. If there are many insignificant model terms (not counting those required to support hierarchy), model reduction may improve your model.

The lack-of-fit test diagnoses how well the full model fit the data. Lack of Fit F-value of 3.31 implies the Lack of Fit is not significant relative to the pure error. There is a 17.7% chance that a “Lack of Fit F-value” this large could occur due to noise.

The contribution percentage of each parameter can be defined as the sum of squares (SS) of a parameter divided by the total SS of all parameters and multiplied by 100. When all the parameters have same degrees of freedom the contribution percentage can be used to determine parameters contribution to the total model. (Akhondi, et al., 2014). Figure 20 shows the contribution of the parameters under study to the proposed model. Back pulsing duration

has the biggest effect, followed by back pulsing pressure and frequency. This is in agreement with the preliminary results obtained by the correlation grid.

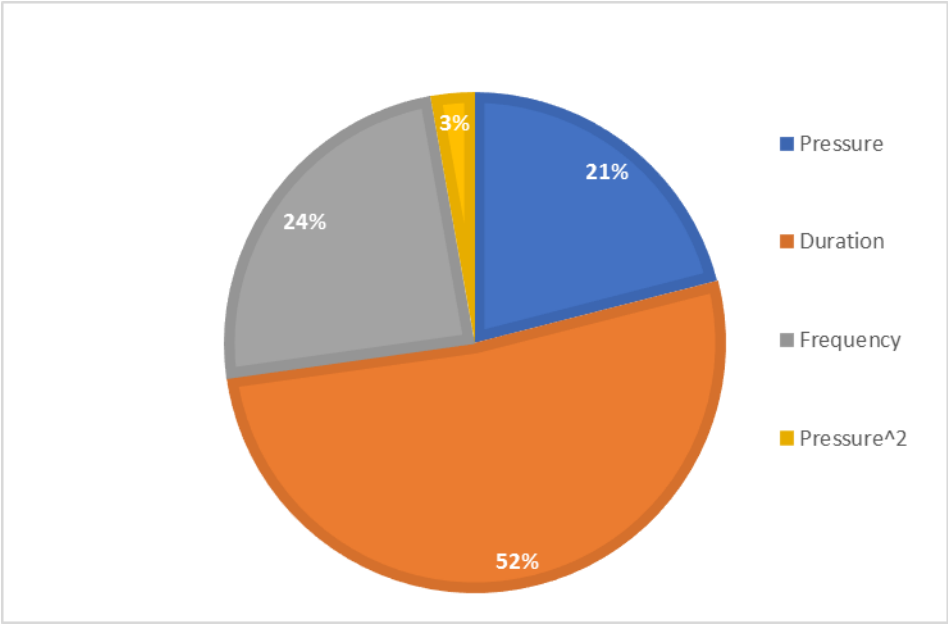

Figure 20- Contribution percentage of parameters to permeate amount

As specified in Table 7, the Predicted R^2 of 0.9254 is in reasonable agreement with the Adjusted R^2 of 0.9588; i.e. the difference is less than 0.2. The adjusted R^2 is a modified version of R^2 that has been adjusted for the number of parameters in the model and represents a better assessment of the model's fit compared to R^2 itself. The predicted R^2 indicates how well a regression model predicts responses for new observations. Low values of Predicted R^2 show a model that fits the original data but is less capable of providing valid predictions for new observations.

Adequate precision measures the signal to noise ratio. It compares the range of the predicted values at the design points to the average prediction error. A ratio greater than 4 is desirable. The obtained ratio of 29.988 indicates an adequate signal. This model can be used to navigate the design space.

Table 7-Model fit statistics

Std. Dev.	11.75	R^2	0.9685
Mean	306.67	Adjusted R^2	0.9588

C.V. %	3.83	Predicted R^2	0.9254
		Adeq Precision	29.9877

Therefore, ANOVA in this case confirms the significance of a quadric model. In other words, the system under study is adequately modeled by the linear and quadric terms in the design space and terms of higher order are not significant.

3.2.2.2 Model Statistical Properties Diagnosis

The most important diagnostic is the normal probability plot of the residuals. Data points should be approximately linear in the normal probability plot. A non-linear pattern (such as an S-shaped curve) indicates non-normality in the error term, which may be corrected by a transformation (Montgomery, et al., 2003). In this case, Figure 21, the data points are approximately linear, confirming the normal distribution of the residuals with a constant variance.

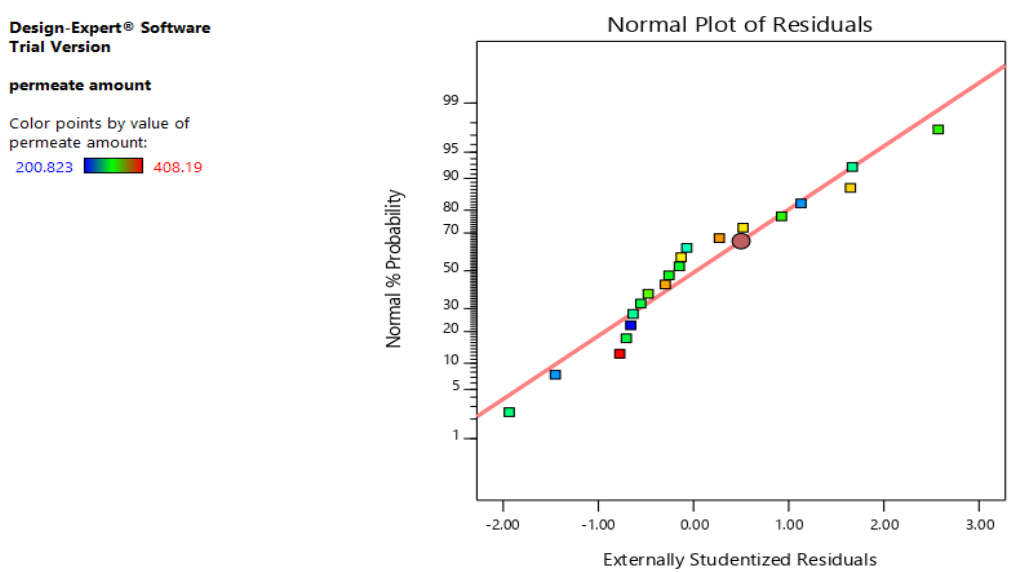

Figure 21-Normal probability plot

Figure 22 shows the actual data points versus the predicted response variable. The data points lie well close to the perdition plot, further confirming that the proposed model is well fitted to describe the design space.

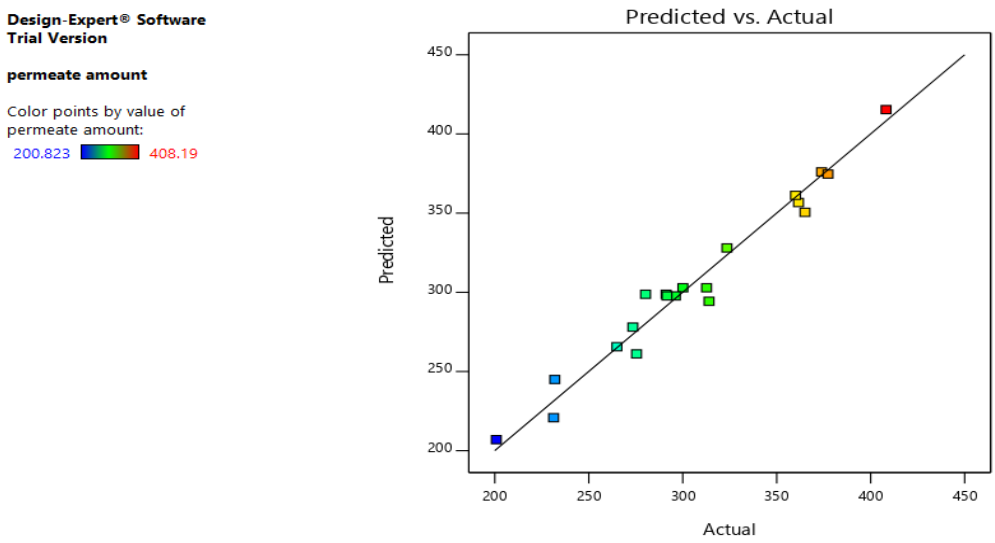

Figure 22-Actual vs predicted response variable

The response surface is shown in Figure 23. Figure 23, is a 3D plot of permeate amount vs. back pulsing duration and pressure at fixed frequency of 75 seconds. The response surface is nearly linear; in agreement with the model equation where it is defined by three linear terms and one quadratic term. The slight curvature observed in the plot is due to the quadric term of pressure in the model equation.

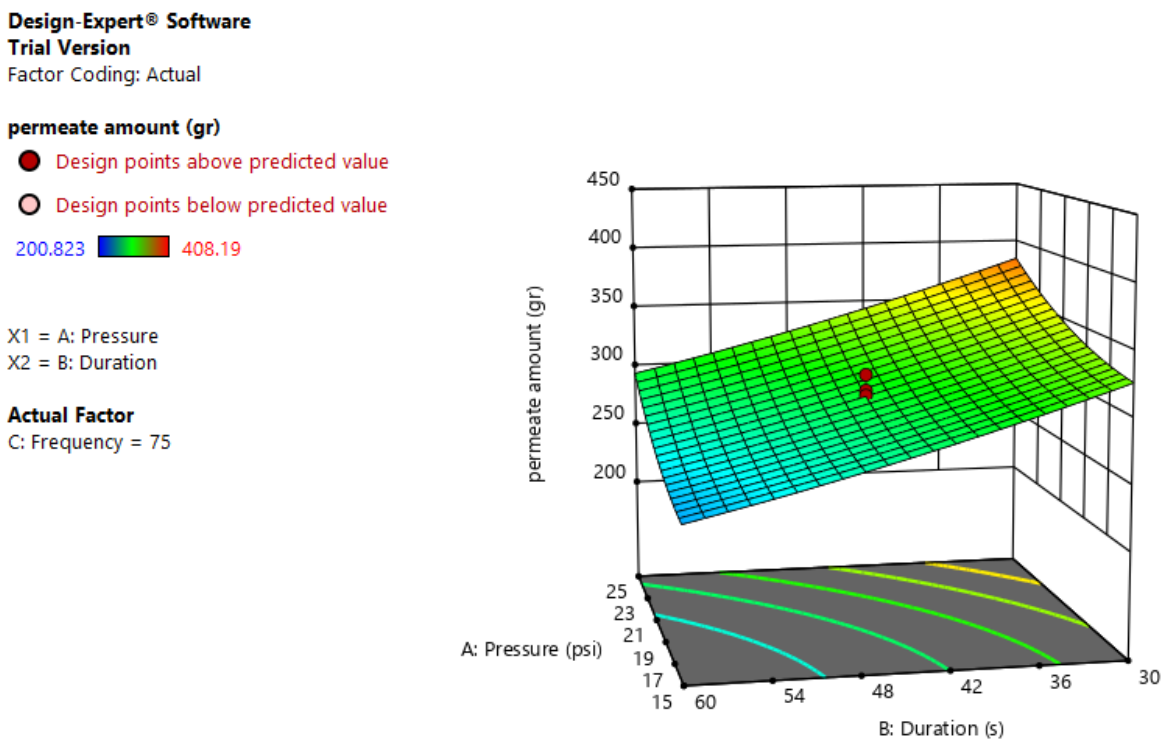

Figure 23-3D presentation of permeate amount vs back pulsing pressure and duration at frequency=75s.

3.2.3 Optimization

The parameter values for maximum permeate amount in the region of study was found by Design-Expert software as follow: Pressure=25psig, Duration=30s, Frequency=90s. The maximum permeate amount obtained was 411.24 grams. This is depicted by Figure 24 where parameters value for maximum permeate amount is determined on a graph of corresponding parameter vs permeate amount. Design-Expert uses an optimization method developed by Derringer and Suich described by Myers, et al. (2016) in Response Surface Methodology, 3rd edithion. (Myers, et al., 2016)

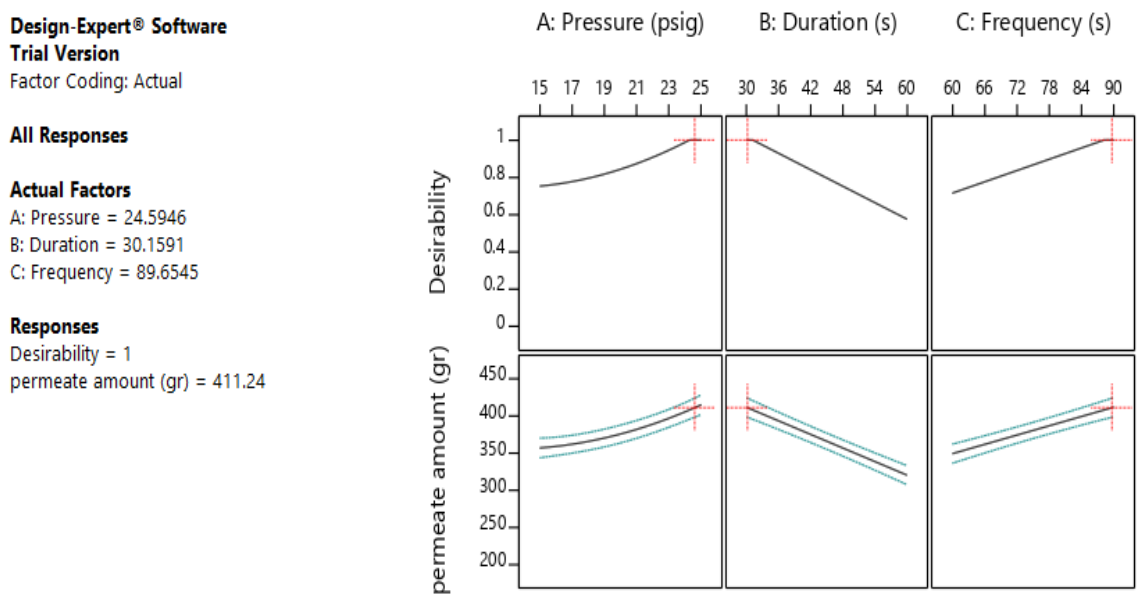

Figure 24-Parameter values for maximum permeate amount.

Figure 25, depicts a comparison of cumulative permeate amount for three different runs. First, a filtration run of model wastewater without air back pulsing for duration of 10 minutes. Second a filtration run at optimum parameter levels determined by RSM analysis and third a filtration run at pressure=15psig, duration=60s, frequency=60s. The total permeate amount obtained using back pulsing assisted filtration process at optimum parameters' levels is 83% higher than the one obtained without back pulsing.

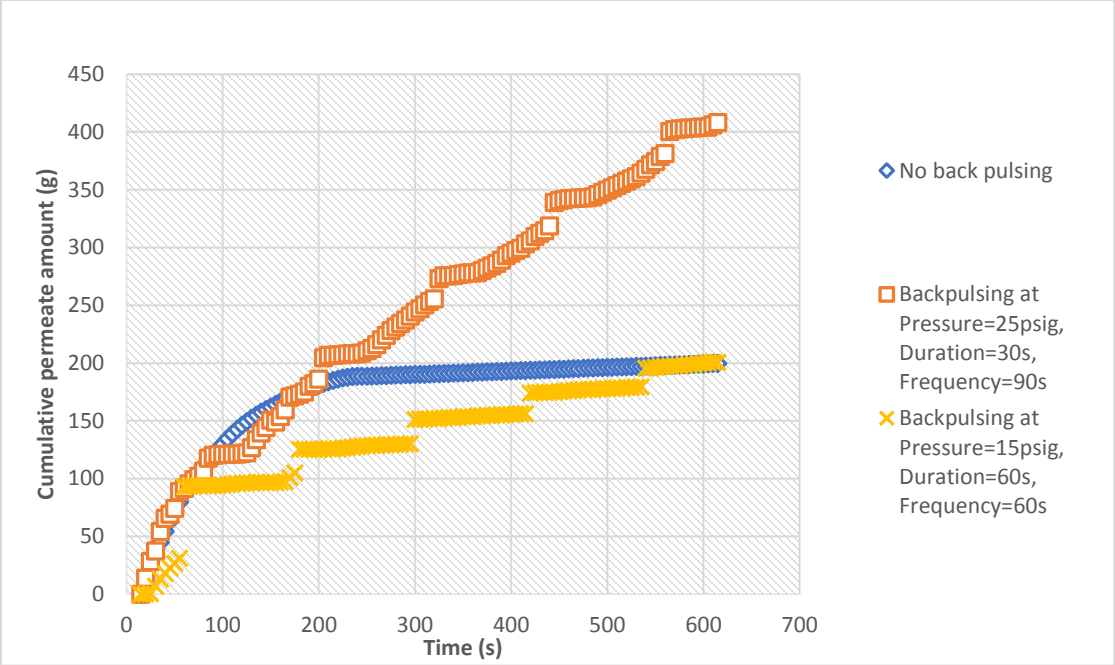

Figure 25- cumulative permeate amount vs time.

Further, the permeate collection rate has remained high throughout the run. This can be seen by nearly constant slope of the corresponding plot. The permeate amount obtained at pressure=15psig, duration=60s, frequency=60s shows no improvement compared to the run without back pulsing. These operating conditions in this run is at the lowest level of pressure, lowest level of frequency and highest level of duration in the design space.

3.3 Scanning Electron Microscope Imaging

Images obtained by Scanning Electron Microscope (SEM) imaging for three samples of PVDF membranes are shown below. Figure 26 presents an image of a fresh membrane. It can be seen that the fibres are clearly visible and free of any deposits on or within the pores.

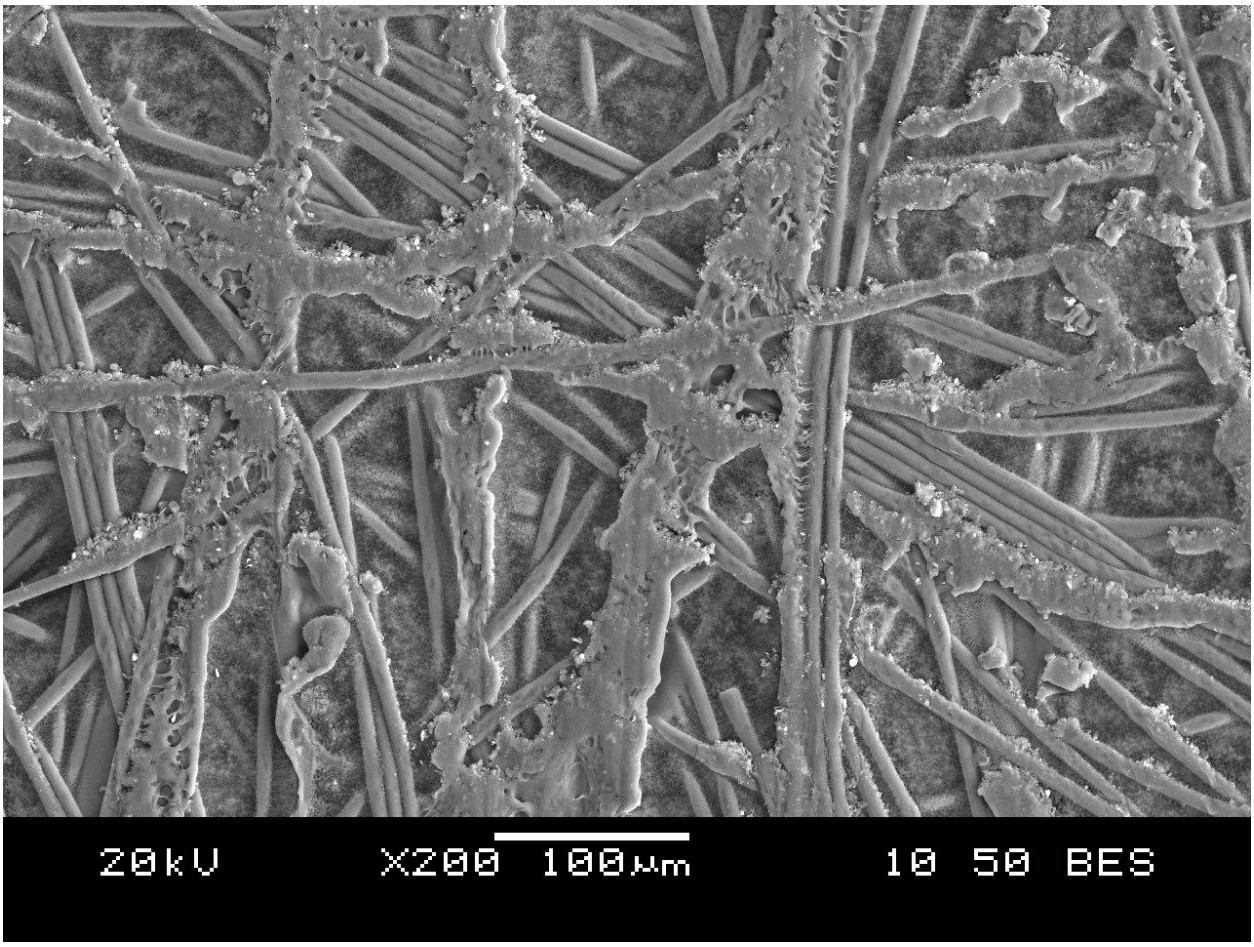

Figure 26-SEM image of fresh PVDF membrane

Figure 27, shows an image of the membrane after 10 minutes of filtration without any back pulsing. It is apparent that the space between the fibers are filled and clogged; despite the first image, fibers are not visible beyond the top surface. Also, deposits are seen on the surface of the membrane.

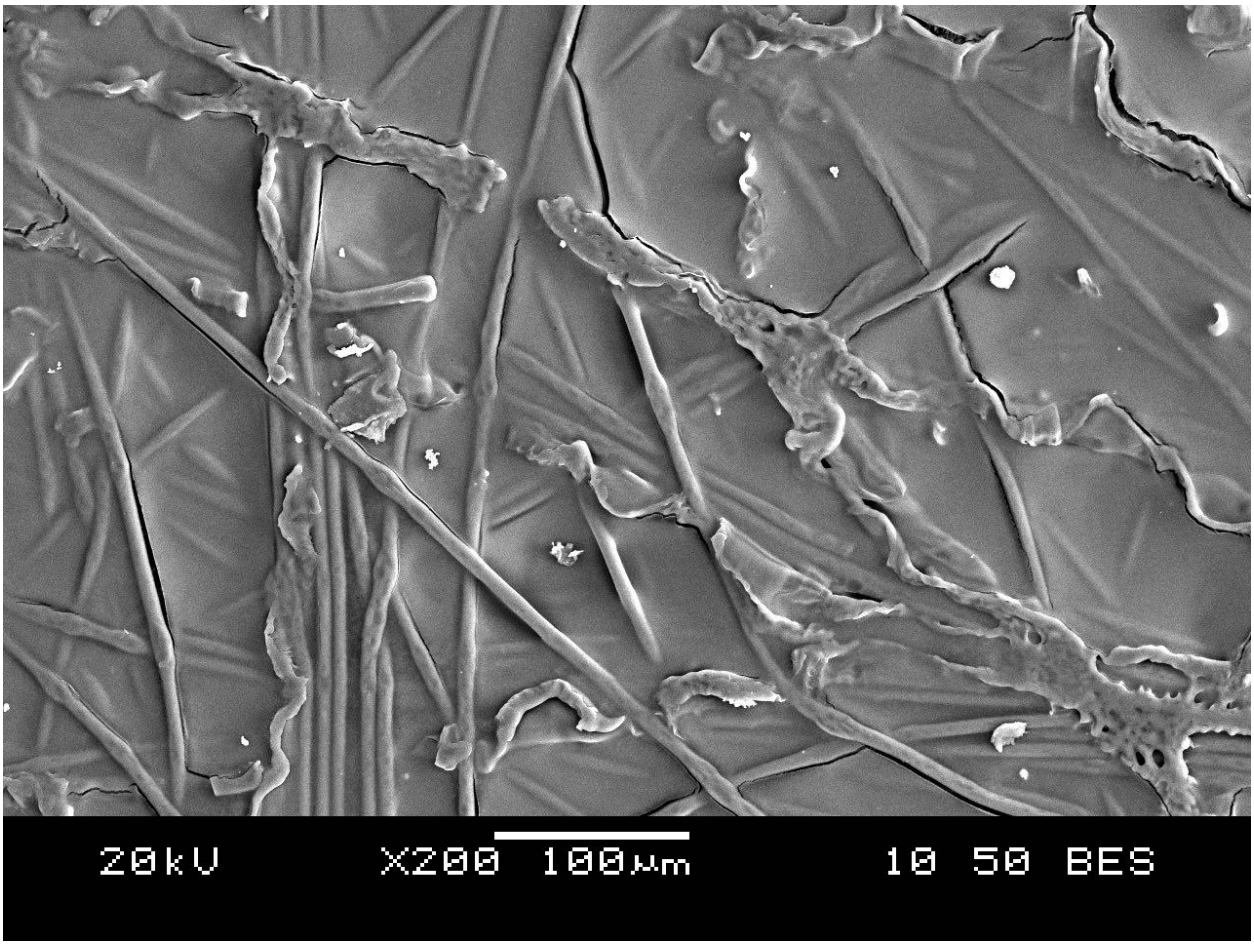

Figure 27-SEM image of PVDF membrane after 10 minutes of filtration with model feed and no back pulsing.

Figure 28 presents an SEM image of the PVDF membrane after 10 minutes of filtration with model feed and back pulsing performed at optimum operating condition of $p_b = 25\ psig$, $d = 30\ s$ and $f = 90\ s$. It can be seen that the pores of the membrane are still blocked, however at the membrane surface more fibers are visible that is indicative of thinner cake fouling cake layer. These results specify that back pulsing has been effective in interrupting concentration polarization and reducing surface deposit, however, it could do little in unclogging the pores and detaching the particles. As proposed by previous researcher(s); due to low density of air in a gas sparged systems, the applied shear force is not strong enough to detach particles completely.

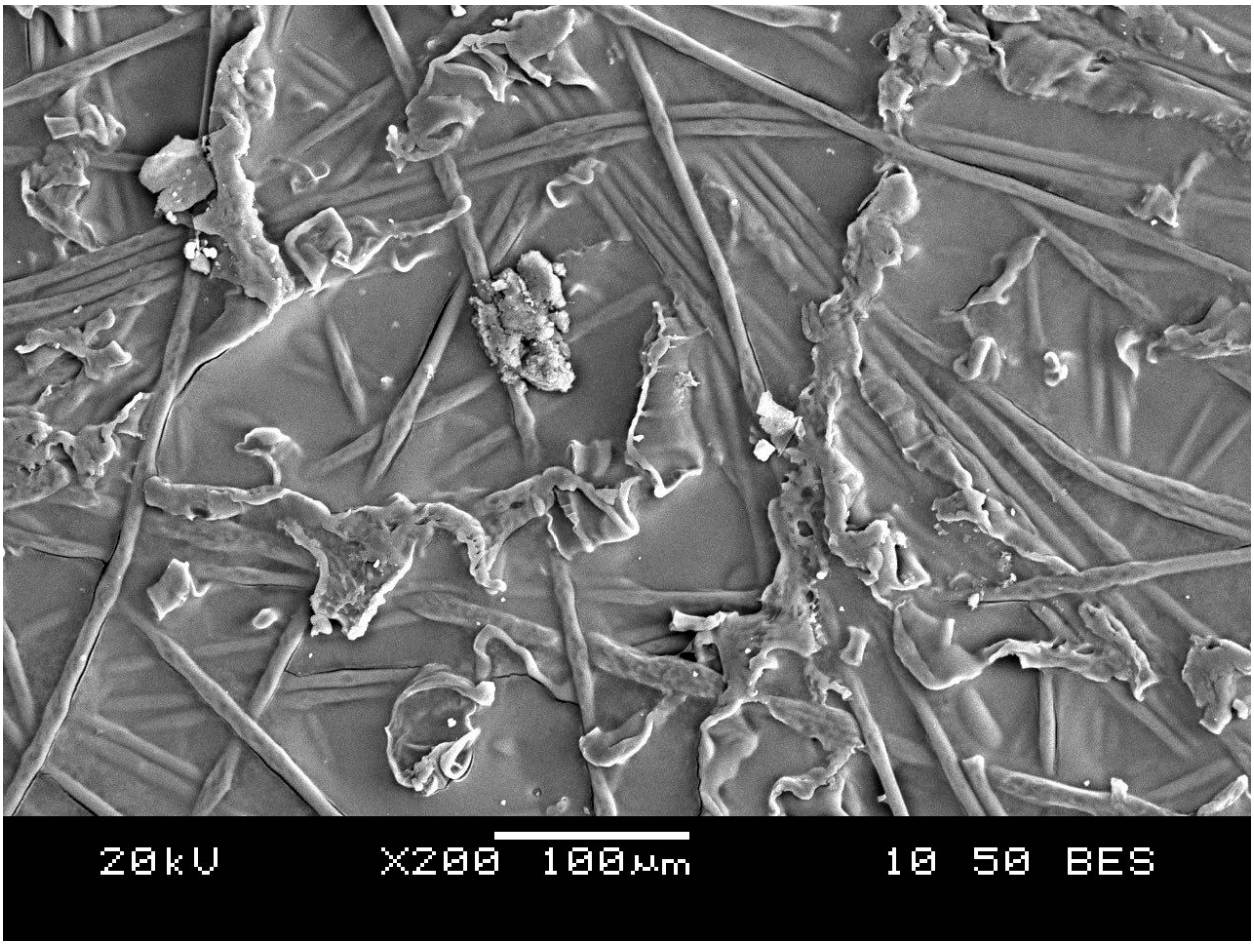

Figure 28- SEM image of the PVDF membrane after 10 minutes of filtration with model feed and back pulsing.

Conclusion

As suggested by RSM analysis of the results, the permeate amount as the response variable is almost a linear function of back pulsing pressure, duration and frequency. The permeate amount is directly proportional to back pulsing pressure and frequency and inversely proportional to back pulsing duration. In other words, high pressures of air in short durations of back pulsing can improve the filtration process and will result in higher amounts of permeate. However, it is anticipated that beyond the region studied, very high frequency would not be helpful. Too high frequency means less back pulsing time over a prolonged filtration process, and this might result in an insufficient cleaning effect of air back pulsing.

The maximum permeate amount obtained using back pulsing assisted filtration process was 83% higher than the one obtained without back pulsing.

The improvement of filtration process could be attributed to two factors: First, as the back pulsing was performed very close to the beginning of the filtration cycle, it alleviates the compaction of foulants and the formation of cake layer on the membrane surface. Therefore, the rejected material was kept in a dispersed phase and carried away by the reject stream (lower concentration polarization). Second, the membrane pores where unclogged of the particles by pressurized air. However, as proposed by previous researcher(s), the effect of the first factor is more pronounced than the second factor in a gas sparging system. Due to low density of air, the applied shear force is not strong enough to detach particles completely.

Recommendations

It is recommended that the effect of parameters beyond the current design space to be investigated to see if a linear relationship, similar to the one obtained, is descriptive of the response variable over the entire space of the independent variables. As suggested by the results high pressure pulses in short durations are more effective in improvement of filtration process. This could be investigated by setting pulsing duration to lower than 30 seconds and back pulsing frequency (filtration time) higher than 75 seconds.

Further, bigger changes in parameter levels would allow for better observation of their effect on response variable as parameter's effects (statistical influence of statistical factors) would be more easily distinguished from random error.

In addition, air containing ozone at a low-concentration can be used instead of pure air for the purpose of back pulsing. Ozonation has been widely applied for membrane fouling mitigation due its ability to directly oxidize organic foulants on membrane surface and/or in membrane pores and to improve membrane hydrophilicity (Tangab, et al., 2018).Back pulsing with ozone laden air can provide back pulsing and ozonation advantages at the same time, given that the membrane doesn't disintegrate by zone.

Appendix A

Table 8-RSM Experimental Data. Runs 1 to 7

Time (s)	Run 1	Run 2	Run 3	Run 4	Run 5	Run 6	Run 7
15	0.0	0.0	0.0	0.0	0.0	0.0	0.0
20	1.8	10.6	2.1	13.8	21.2	13.8	9.3
25	6.5	28.5	6.8	25.8	34.0	28.1	20.1
30	16.1	39.3	11.7	34.3	41.1	37.2	29.2
35	21.5	44.6	21.0	40.9	46.9	54.2	36.8
40	24.3	53.1	27.8	47.1	52.0	65.4	44.1
45	26.6	56.5	33.8	52.1	57.1	69.1	51.0
50	30.1	58.8	36.7	56.8	61.0	74.1	57.5
55	35.4	66.3	39.5	79.1	64.6	88.7	63.6
60	37.3	87.0	48.1	82.7	68.3	91.7	69.8
65	37.7	88.1	51.6	83.1	71.8	95.4	75.1
70	39.8	88.8	54.2	83.7	96.1	99.0	78.7
75	46.8	89.1	83.1	83.7	99.0	102.2	81.9
80	50.1	90.2	83.1	83.7	99.3	106.4	84.9
85	50.9	90.8	83.1	84.2	99.5	117.5	101.3
90	62.5	91.3	83.4	84.9	100.4	120.2	109.1
95	63.7	92.3	83.3	85.5	101.1	120.7	109.2
100	64.7	93.3	83.6	85.8	101.7	120.8	109.3
105	65.6	94.2	83.4	85.9	102.0	120.9	109.7
110	66.2	108.1	83.1	86.3	102.7	121.1	110.2
115	67.1	114.4	83.3	87.2	102.8	121.1	110.3
120	67.6	116.5	83.0	87.8	103.1	121.7	110.9
125	68.2	118.1	83.1	88.1	103.4	122.3	111.4
130	68.8	119.2	84.7	89.2	107.8	126.8	113.8
135	69.9	120.2	86.4	94.7	112.1	133.7	116.3
140	70.3	121.1	88.0	99.7	116.0	139.4	118.7
145	71.1	122.1	91.4	103.2	119.0	144.2	121.1
150	71.7	142.6	94.7	106.5	121.9	150.6	123.6
155	72.0	143.0	97.1	110.5	124.9	148.9	126.0
160	73.7	143.6	99.2	114.4	127.4	153.6	128.5
165	75.1	144.1	101.3	117.1	129.2	159.4	130.9
170	75.2	145.1	103.2	119.4	131.3	170.6	133.3
175	77.8	145.9	105.0	136.3	133.8	171.6	135.7
180	83.8	146.5	106.7	140.5	135.8	173.1	138.2
185	86.0	147.1	108.5	140.9	137.4	174.9	140.6
190	88.1	148.0	110.1	141.3	160.3	180.0	143.1
195	89.8	148.9	140.3	141.9	163.0	182.2	145.5

200	95.3	149.8	140.8	141.8	163.8	186.0	147.8
205	98.3	150.7	140.6	142.4	163.8	204.6	168.2
210	100.6	151.8	141.0	143.2	164.4	206.4	175.7
215	102.9	161.3	141.0	143.4	164.6	206.8	176.2
220	104.9	164.0	140.9	143.4	164.6	207.1	176.2
225	107.1	165.4	141.4	143.8	164.7	207.3	176.1
230	113.8	166.5	141.6	144.4	164.7	207.9	176.2
235	116.1	167.6	141.9	144.7	165.0	208.1	176.3
240	127.5	182.6	141.9	145.0	165.9	208.0	176.6
245	127.9	183.6	141.6	145.6	166.3	208.8	177.1
250	128.2	184.4	143.3	146.8	166.9	210.8	179.5
255	128.8	185.5	144.9	147.9	167.5	212.5	182.0
260	130.0	186.3	146.5	149.0	168.2	215.9	184.5
265	130.7	186.8	148.1	152.6	170.1	220.2	187.0
270	131.4	187.9	149.8	154.8	171.4	224.1	189.4
275	132.6	188.3	151.5	158.2	175.4	228.0	191.8
280	133.0	189.3	153.1	161.8	177.0	231.3	194.2
285	133.6	190.3	154.9	164.9	179.8	234.1	196.7
290	134.2	191.2	156.4	168.0	180.7	237.3	199.1
295	134.7	192.1	158.1	181.9	183.4	240.5	201.5
300	135.4	193.1	160.7	186.3	184.4	244.3	203.9
305	135.7	193.9	163.2	186.7	187.0	247.0	206.4
310	137.4	194.9	165.3	187.3	205.4	250.2	208.8
315	139.2	195.9	189.6	187.7	209.2	253.3	211.2
320	141.0	196.7	189.8	187.8	209.6	255.6	213.6
325	144.0	197.7	190.1	187.9	210.5	273.1	228.5
330	147.5	218.7	190.6	187.9	210.6	275.6	235.5
335	149.4	219.1	191.0	188.8	210.9	275.5	235.7
340	151.4	219.5	190.6	189.0	211.2	275.9	236.4
345	153.2	220.0	190.8	189.5	211.4	276.5	237.2
350	155.0	220.2	191.3	189.7	211.8	277.2	237.6
355	161.9	221.2	191.3	190.5	211.8	277.9	237.9
360	164.2	222.2	191.6	190.7	212.2	278.0	237.8
365	166.2	222.7	191.7	191.4	213.1	278.4	238.0
370	168.0	223.7	193.5	192.6	213.4	280.3	240.4
375	169.8	224.6	195.1	193.7	214.5	282.2	243.0
380	171.5	225.6	196.8	194.8	215.0	284.2	245.4
385	173.4	226.5	198.4	195.9	215.7	286.2	247.9
390	190.3	227.4	200.1	202.9	216.4	289.2	250.3
395	191.0	228.3	201.9	204.8	218.6	293.0	252.8
400	192.2	229.3	203.4	206.1	219.9	295.2	255.3
405	192.9	230.3	205.1	207.4	223.0	297.3	257.7
410	194.0	231.1	206.7	208.5	224.6	299.3	260.2

415	194.9	232.2	208.4	224.0	225.6	303.3	262.6
420	195.5	249.4	210.0	228.9	228.1	305.7	265.0
425	196.4	250.3	211.6	229.0	229.0	309.7	267.5
430	196.7	250.9	213.2	229.2	245.3	312.3	269.9
435	197.7	251.9	236.8	229.2	249.0	314.5	272.3
440	198.6	252.8	236.9	229.6	249.5	318.6	274.6
445	199.3	253.5	237.0	229.9	250.3	339.0	287.9
450	199.6	253.7	236.9	230.4	250.9	340.7	295.0
455	200.0	254.3	236.9	230.4	251.2	341.4	295.0
460	201.8	255.3	236.8	230.6	251.8	342.2	295.6
465	203.6	256.3	236.5	230.6	251.8	342.5	296.5
470	205.3	257.2	236.3	230.9	252.4	342.8	296.7
475	207.0	258.2	236.9	231.5	253.0	343.1	296.8
480	208.8	259.2	236.5	232.0	253.4	343.2	297.6
485	211.3	260.0	236.5	232.9	253.5	343.9	297.6
490	215.9	261.0	238.2	234.1	254.2	345.8	300.0
495	218.2	262.0	239.9	235.2	254.8	347.8	302.5
500	220.0	262.9	241.4	236.4	255.5	349.6	305.0
505	221.9	263.8	243.1	237.5	256.1	351.6	307.4
510	223.7	281.5	244.7	238.5	256.8	353.6	309.9
515	230.5	282.0	246.4	240.4	257.4	355.6	312.3
520	234.2	282.9	248.0	241.9	258.1	357.4	314.8
525	236.4	283.5	249.6	243.3	258.9	359.4	317.2
530	238.3	284.4	251.5	246.0	259.6	361.3	319.6
535	240.2	284.8	253.0	260.7	260.3	364.4	321.9
540	250.7	285.6	254.7	266.6	260.9	367.7	324.4
545	251.2	286.8	256.3	267.3	267.7	371.7	326.9
550	252.2	287.6	258.0	267.8	281.2	374.4	329.2
555	252.5	288.7	279.8	268.3	285.2	378.9	331.7
560	253.2	289.8	279.8	268.4	285.3	381.3	334.1
565	254.1	290.6	279.9	269.2	285.6	400.5	346.9
570	255.1	291.6	279.6	269.4	286.2	402.1	353.9
575	255.7	292.6	279.7	269.9	286.2	402.6	354.4
580	256.8	293.5	279.6	270.4	286.6	403.0	354.9
585	257.8	294.4	279.8	271.0	287.3	403.5	355.4
590	258.7	295.4	280.0	271.7	288.0	403.5	356.0
595	259.8	296.4	279.7	272.2	288.2	404.1	356.8
600	260.9	312.1	280.2	272.9	289.1	404.3	356.8
605	261.5	312.5	280.2	273.1	289.8	404.3	357.1
610	263.2	313.7	280.2	274.2	290.5	406.2	358.5
615	265.0	314.0	280.2	275.4	291.2	408.2	360.0

Table 9- RSM Experimental Data. Runs 8 to 14

Time (s)	Run 8	Run 9	Run 10	Run 11	Run 12	Run 13	Run 14
15	0.0	0.0	0.0	0.0	0.0	0.0	0.0
20	0.3	25.2	2.4	6.1	8.4	1.9	5.8
25	0.5	39.3	7.6	22.0	20.9	3.8	27.6
30	6.9	52.4	12.8	34.5	27.1	5.8	40.2
35	12.8	55.6	22.5	42.6	34.4	7.7	51.1
40	17.9	62.5	29.6	48.8	37.9	9.6	56.3
45	22.5	65.5	36.0	55.4	41.7	12.5	62.0
50	26.7	73.6	39.3	60.3	50.9	32.3	65.8
55	30.8	97.8	42.4	64.4	54.4	32.9	70.2
60	92.9	98.3	51.5	68.3	57.3	33.5	73.8
65	93.2	98.4	55.3	72.9	59.7	34.1	78.1
70	93.4	98.5	58.2	76.8	62.0	34.2	80.9
75	93.7	99.2	87.5	100.7	64.1	34.8	104.5
80	93.9	99.5	87.8	100.2	70.5	34.8	105.0
85	93.9	99.5	88.0	100.0	94.9	35.0	105.3
90	93.8	100.2	88.0	99.6	99.3	35.5	105.7
95	94.2	100.0	88.0	99.6	99.9	36.1	105.8
100	94.4	109.2	87.9	99.9	100.9	36.4	105.9
105	94.7	111.8	88.3	99.9	101.6	37.8	106.5
110	95.4	113.7	88.7	100.0	102.7	39.4	106.3
115	95.7	120.0	89.4	100.4	103.5	45.1	106.9
120	96.0	122.7	89.2	100.7	104.3	54.3	107.5
125	96.2	124.5	89.2	100.7	105.2	56.9	108.0
130	96.0	125.9	91.2	102.3	106.1	59.0	108.9
135	96.7	132.3	93.1	104.4	107.4	60.8	109.7
140	96.7	134.7	95.1	106.5	107.8	62.4	110.6
145	96.5	159.1	98.7	110.7	108.6	79.8	114.0
150	96.6	158.9	102.3	114.0	109.0	79.9	116.3
155	96.5	158.8	105.1	116.1	109.9	79.7	118.0
160	96.7	159.6	107.4	118.7	111.5	80.1	119.7
165	97.5	160.2	109.9	120.8	113.2	79.9	121.2
170	101.0	160.9	112.0	122.8	115.5	79.6	122.2
175	104.8	161.7	114.2	124.3	118.2	79.6	123.2
180	125.5	161.7	116.1	131.3	120.3	79.9	129.5
185	125.4	162.2	118.2	134.9	122.3	79.9	132.0
190	125.3	163.2	120.1	137.9	126.7	80.3	133.7
195	125.2	165.6	150.6	161.3	129.6	80.6	156.1
200	125.2	168.3	151.0	161.3	131.9	82.0	156.0
205	125.7	169.9	151.3	161.6	134.0	83.6	156.2
210	125.8	171.3	151.3	161.1	135.9	85.1	156.8
215	125.7	176.8	152.0	160.9	139.8	86.5	157.4

220	125.6	179.1	152.1	161.1	144.9	88.0	157.6
225	126.1	180.9	152.9	160.9	147.9	97.0	158.4
230	126.7	182.2	153.1	160.6	150.2	101.4	159.0
235	127.0	207.7	153.7	160.3	171.5	103.4	158.9
240	127.6	207.7	154.3	159.9	176.5	118.3	159.6
245	128.4	208.2	154.7	160.3	177.0	118.2	159.8
250	128.5	208.9	156.6	162.5	177.8	118.2	160.7
255	128.7	209.2	158.6	164.2	178.5	118.3	161.5
260	128.9	209.0	160.4	166.3	179.8	118.4	162.4
265	129.0	209.7	162.4	167.7	180.7	118.5	163.3
270	129.2	209.7	164.3	169.5	181.8	119.2	164.2
275	129.3	209.7	166.4	171.6	182.3	119.2	165.0
280	129.5	210.8	168.2	172.8	183.5	119.3	165.8
285	129.7	211.8	170.3	174.2	184.7	120.0	166.8
290	129.9	212.9	172.1	175.6	185.3	120.0	167.6
295	130.1	214.9	174.1	177.7	186.5	121.4	168.4
300	151.2	216.9	177.0	180.6	187.3	122.9	170.7
305	151.5	218.6	179.8	183.5	187.8	124.4	173.1
310	151.4	219.9	182.2	185.7	189.4	125.9	174.5
315	151.8	221.1	206.8	208.2	191.0	127.4	196.2
320	152.0	222.2	206.9	208.2	192.6	128.8	196.6
325	152.0	249.3	207.3	208.5	194.2	130.3	197.1
330	152.5	249.1	207.8	208.4	195.9	131.8	197.0
335	152.7	249.5	208.2	208.0	198.1	152.7	197.4
340	152.9	249.7	208.0	207.5	200.8	152.7	197.6
345	152.9	250.0	208.7	207.8	202.9	152.6	197.7
350	153.6	250.7	208.5	208.2	204.7	153.0	198.2
355	153.5	251.1	208.5	207.8	206.3	153.2	198.6
360	153.7	251.8	208.6	208.1	208.0	153.9	198.7
365	154.2	252.4	208.8	208.0	209.7	154.0	198.7
370	154.5	253.4	210.9	210.2	211.3	154.3	199.7
375	154.6	254.5	212.8	212.0	213.0	154.3	200.5
380	154.8	255.5	214.8	213.8	222.9	154.2	201.5
385	154.9	256.6	216.7	215.5	241.8	154.0	202.2
390	155.1	260.3	218.7	216.9	246.2	155.5	203.1
395	155.4	263.0	220.8	219.1	247.4	157.0	204.0
400	155.6	264.8	222.6	221.0	248.2	158.5	204.9
405	155.8	266.3	224.6	222.4	249.5	160.0	205.7
410	156.0	267.6	226.5	224.5	249.8	161.5	206.6
415	156.1	290.1	228.5	226.4	251.1	163.1	207.4
420	173.8	289.5	230.4	228.3	252.2	164.5	208.4
425	174.2	289.7	232.3	229.8	252.8	166.0	209.1
430	174.7	290.2	234.2	231.3	253.3	184.5	210.0

435	174.6	290.6	258.1	254.9	254.1	185.1	232.7
440	174.8	290.8	258.3	254.4	255.0	185.2	233.3
445	174.6	290.7	258.9	254.4	255.6	185.4	233.9
450	175.2	290.5	258.8	254.2	256.9	185.4	234.3
455	175.9	290.7	259.5	254.0	257.4	185.2	235.1
460	176.0	291.7	259.5	253.9	259.0	185.8	235.8
465	176.0	292.7	259.4	253.7	260.5	186.1	235.8
470	176.8	293.9	260.0	253.8	262.1	186.1	236.3
475	176.8	294.9	259.8	253.7	263.8	186.3	237.1
480	177.0	296.0	259.7	253.2	265.4	186.3	237.2
485	177.1	297.0	260.2	252.9	267.0	187.9	237.5
490	177.4	298.1	262.2	254.4	268.6	189.3	238.3
495	177.7	302.1	264.1	256.3	271.8	190.8	239.1
500	177.9	304.6	266.0	258.1	274.6	192.4	240.0
505	178.0	326.2	267.9	259.9	276.7	193.8	240.9
510	178.2	325.6	269.9	262.1	278.7	195.3	241.8
515	178.4	325.8	271.8	264.1	280.5	196.9	242.6
520	178.7	325.9	273.8	266.1	282.2	198.3	243.5
525	178.9	326.4	275.6	267.4	283.7	218.2	244.4
530	179.2	326.4	277.8	268.9	285.4	218.7	245.2
535	179.3	326.6	279.6	271.2	304.9	219.1	246.1
540	195.5	326.5	281.6	273.3	311.9	219.7	246.9
545	195.6	327.3	283.5	275.4	312.8	219.6	247.8
550	196.4	328.4	285.5	277.3	313.2	219.4	248.6
555	196.8	329.4	307.6	299.3	314.4	219.6	270.0
560	197.1	330.5	307.7	299.2	314.7	219.4	269.9
565	197.1	331.6	308.3	298.9	315.5	219.3	270.7
570	197.8	332.7	308.4	298.9	316.3	219.5	271.2
575	197.6	333.8	308.4	298.8	316.7	220.0	271.0
580	198.2	334.7	308.7	299.1	317.1	221.5	271.4
585	198.7	335.8	309.1	298.9	317.8	222.9	271.3
590	198.8	337.6	309.5	298.5	318.1	224.5	271.2
595	199.5	362.2	309.4	298.9	319.4	226.0	271.8
600	199.8	361.1	310.2	298.5	320.7	227.4	271.9
605	200.3	361.2	310.3	298.1	321.5	228.9	271.7
610	200.6	361.0	312.4	300.1	323.1	230.5	272.6
615	200.8	361.6	312.7	300.1	323.5	231.9	273.5

Table 10- RSM Experimental Data. Runs 15 to 20

Time (s)	Run 15	Run 16	Run 17	Run 18	Run 19	Run 20
15	0.0	0.0	0.0	0.0	0.0	0.0
20	2.1	4.4	18.0	9.4	12.8	2.1
25	6.8	21.9	50.3	22.2	24.2	6.8
30	11.7	36.7	57.7	25.5	31.1	11.7
35	20.9	42.1	66.6	28.1	37.7	21.0
40	27.7	50.0	71.7	37.1	42.9	27.7
45	33.8	54.9	81.1	40.6	47.1	33.8
50	36.6	63.7	85.9	43.4	53.6	36.6
55	39.4	68.6	91.3	46.0	58.4	39.4
60	48.0	73.1	96.3	48.4	62.6	48.1
65	51.5	77.7	102.0	50.7	66.4	51.5
70	54.1	86.3	111.5	66.8	70.0	54.1
75	82.9	103.8	131.1	71.8	73.5	83.0
80	83.6	104.2	131.5	71.6	80.3	83.4
85	83.8	105.4	131.5	71.8	84.8	83.7
90	84.0	106.6	132.2	72.3	88.9	84.5
95	84.1	107.5	132.7	72.5	96.5	85.5
100	84.3	108.5	133.4	73.1	105.3	86.7
105	84.8	112.0	133.9	73.6	106.4	87.7
110	85.4	115.6	134.3	74.0	107.4	88.3
115	85.7	119.1	135.1	74.3	107.9	88.9
120	86.4	122.6	135.8	74.1	109.2	89.4
125	86.2	126.2	136.4	73.9	109.8	90.6
130	87.9	129.7	138.4	74.2	110.8	92.3
135	89.5	133.1	140.4	74.5	111.9	93.9
140	91.2	136.7	142.4	74.4	112.8	95.6
145	94.5	146.3	146.8	74.8	113.4	98.9
150	97.8	154.3	150.3	75.2	114.1	102.2
155	100.2	158.3	153.1	77.0	117.1	104.6
160	102.3	162.0	155.9	78.9	120.0	106.7
165	104.4	165.8	158.5	80.8	123.0	108.8
170	106.3	181.5	160.6	82.6	125.9	110.7
175	108.1	182.8	162.7	84.4	128.8	112.5
180	109.8	183.3	170.1	93.8	131.9	114.2
185	111.5	183.7	173.7	96.8	134.8	115.9
190	113.2	184.9	176.6	99.4	137.8	117.6
195	143.3	186.0	200.0	101.6	140.7	147.7
200	143.9	189.5	200.4	103.6	143.7	148.3
205	144.5	193.0	200.5	105.4	146.6	148.4
210	144.6	196.5	201.1	107.4	149.5	148.6
215	145.3	200.2	201.5	121.8	152.6	148.9

220	145.4	203.7	201.9	121.2	165.5	149.2
225	145.8	207.1	202.5	121.9	170.4	149.7
230	146.1	210.7	203.1	122.0	173.9	149.7
235	146.1	214.2	203.6	121.7	177.2	149.7
240	146.3	217.7	204.3	122.2	180.6	149.9
245	146.8	221.3	204.4	122.7	192.2	150.1
250	148.4	224.7	206.4	122.9	192.3	151.8
255	150.1	228.3	208.4	122.9	192.7	153.4
260	151.6	231.8	210.3	122.9	193.3	155.0
265	153.3	252.3	212.3	122.7	194.0	156.6
270	154.9	252.8	214.3	123.0	194.2	158.3
275	156.7	253.8	216.3	123.5	194.9	160.0
280	158.2	254.8	218.2	123.3	195.0	161.6
285	160.0	255.7	220.2	123.7	195.5	163.3
290	161.5	256.0	222.1	124.4	196.1	164.9
295	163.2	259.6	224.1	124.6	196.7	166.5
300	165.8	263.1	227.5	126.5	199.6	169.2
305	168.3	266.7	231.0	128.3	202.6	171.6
310	170.4	270.3	233.4	130.1	205.6	173.8
315	194.7	273.8	256.3	132.0	208.5	198.0
320	195.0	277.3	256.6	134.0	211.5	198.0
325	195.3	280.8	257.3	135.7	214.5	198.2
330	195.0	284.3	258.0	137.7	217.4	198.2
335	195.3	287.9	258.9	139.4	220.3	198.1
340	195.9	291.4	259.5	141.3	223.3	197.9
345	195.9	294.9	259.6	143.2	226.3	197.9
350	196.1	298.5	260.2	145.0	229.2	198.5
355	196.7	302.0	261.1	146.9	232.2	198.8
360	196.9	322.2	262.1	164.7	235.2	199.2
365	197.1	323.5	262.7	170.0	246.2	199.6
370	198.8	324.7	264.8	170.5	250.8	201.4
375	200.5	325.2	266.7	170.8	254.1	203.0
380	202.1	326.0	268.8	170.7	257.3	204.7
385	203.8	327.2	270.7	170.6	260.4	206.3
390	205.4	330.8	272.6	171.1	271.2	208.0
395	207.3	334.4	274.6	171.4	271.6	209.8
400	208.7	337.9	276.6	171.6	271.8	211.3
405	210.4	341.5	278.6	172.1	271.7	212.9
410	212.0	345.0	280.6	172.2	271.7	214.6
415	213.7	348.5	282.4	172.3	272.4	216.2
420	215.3	352.1	284.5	172.4	272.7	217.9
425	216.9	355.6	286.4	172.4	272.9	219.4
430	218.5	359.1	288.4	172.9	272.7	221.1

435	242.1	362.6	312.2	173.3	273.3	244.6
440	241.9	366.1	312.7	173.6	273.0	245.2
445	242.2	369.6	313.5	175.4	276.0	245.5
450	242.1	373.2	313.7	177.4	279.0	245.9
455	242.4	394.1	314.3	179.2	281.9	245.8
460	242.8	394.9	314.8	181.1	284.8	246.0
465	242.6	396.2	315.3	182.9	287.8	246.7
470	242.8	396.7	315.7	184.8	290.7	247.0
475	243.0	397.9	316.0	186.7	293.7	246.8
480	243.2	398.3	316.3	188.4	296.7	247.4
485	243.1	402.0	316.8	190.3	299.7	247.1
490	244.8	405.6	318.7	192.1	302.6	248.8
495	246.4	409.3	320.6	194.0	305.5	250.4
500	248.0	412.8	322.6	195.9	308.5	252.0
505	249.6	416.3	324.6	212.5	311.5	253.6
510	251.3	420.0	326.6	217.7	314.4	255.3
515	252.9	423.5	328.6	217.8	317.4	256.9
520	254.6	427.1	330.5	217.6	320.4	258.6
525	256.1	430.6	332.5	217.6	323.4	260.1
530	258.0	434.1	334.4	217.5	326.2	262.0
535	259.5	437.7	336.5	217.9	345.8	263.5
540	261.2	441.2	338.4	218.0	345.9	265.2
545	262.8	444.7	340.3	217.9	345.8	266.8
550	264.5	465.6	342.3	218.2	345.6	268.5
555	286.3	466.2	364.8	218.9	345.9	290.3
560	286.7	467.0	365.6	219.1	346.6	290.8
565	286.7	467.9	366.0	219.5	346.4	290.9
570	287.0	469.1	366.1	220.2	346.1	290.7
575	287.6	470.3	366.7	220.0	346.3	291.1
580	287.6	473.9	367.4	220.2	346.6	291.5
585	287.6	477.3	368.2	220.1	347.1	292.2
590	287.4	480.9	368.6	222.0	350.1	292.3
595	287.9	484.4	368.7	223.9	353.1	292.6
600	287.9	488.0	369.1	225.7	356.0	292.7
605	288.2	491.5	369.9	227.6	359.0	292.7
610	290.0	495.1	371.9	229.4	362.1	294.4
615	291.6	377.3	373.9	231.3	365.0	296.1

Table 11-Experimental data for the runs with no back pulsing

Time (S)	Rep 1	Rep 2	Rep 3
15	0	0	0.0
20	11.3	15.5	10.1
25	24.1	28.3	28.7
30	35.2	40.5	39.9
35	44.8	51.0	50.4
40	54.1	61.3	59.7
45	63.0	71.2	69.6
50	71.5	79.7	78.1
55	79.6	87.9	86.3
60	87.8	97.0	94.4
65	95.1	105.3	100.7
70	100.7	110.9	105.3
75	105.9	116.1	110.5
80	110.9	122.1	116.5
85	115.8	128.0	121.4
90	120.5	133.7	125.1
95	125.3	138.5	128.9
100	129.9	143.1	134.5
105	134.5	147.7	138.1
110	138.8	153.0	143.4
115	142.6	157.8	147.2
120	146.1	161.3	151.7
125	149.2	165.5	155.9
130	152.3	168.5	157.9
135	155.0	172.2	159.6
140	157.4	174.6	162.0
145	159.7	177.9	165.3
150	162.0	180.3	167.7
155	164.1	182.3	170.7
160	166.3	185.5	172.9
165	168.4	188.6	176.0
170	170.3	191.5	176.9
175	172.2	193.4	178.8
180	174.1	195.3	179.7
185	176.0	198.2	182.6
190	177.8	200.0	184.4
195	179.5	201.7	187.1
200	181.0	204.2	189.6
205	182.5	205.8	191.2
210	183.8	207.0	191.4
215	184.9	209.1	193.5

220	186.0	210.2	195.6
225	187.0	212.2	196.6
230	187.6	213.9	198.3
235	188.2	214.4	198.8
240	188.4	214.6	200.0
245	188.5	214.7	200.1
250	188.6	214.8	199.2
255	188.8	216.0	199.4
260	188.9	217.1	199.5
265	189.1	217.3	198.7
270	189.2	218.4	198.8
275	189.3	218.6	199.0
280	189.5	218.7	200.1
285	189.7	219.9	200.3
290	189.8	220.0	200.4
295	189.9	221.1	200.5
300	190.1	221.3	200.7
305	190.2	222.4	200.8
310	190.3	223.5	200.9
315	190.5	223.7	201.1
320	190.7	223.9	201.3
325	190.8	224.0	201.4
330	190.9	225.1	201.5
335	191.0	225.3	200.7
340	191.2	226.4	199.8
345	191.3	226.6	200.0
350	191.5	227.7	199.1
355	191.7	228.9	199.3
360	191.8	229.1	198.5
365	192.0	230.2	198.6
370	192.2	231.4	198.8
375	192.3	231.6	198.0
380	192.5	231.7	197.1
385	192.7	232.9	198.3
390	192.8	234.1	197.5
395	193.0	234.2	197.6
400	193.1	234.4	198.8
405	193.3	235.5	197.9
410	193.4	236.6	199.0
415	193.6	237.8	200.2
420	193.8	239.0	200.4
425	193.9	239.1	201.5
430	194.0	239.2	201.6

435	194.1	239.3	201.7
440	194.3	239.5	201.9
445	194.4	239.7	201.1
450	194.6	239.8	202.2
455	194.7	241.0	201.4
460	194.9	242.1	201.5
465	195.1	242.3	201.7
470	195.3	242.5	202.9
475	195.4	242.6	203.0
480	195.6	242.8	203.2
485	195.7	244.0	203.4
490	195.9	244.1	202.5
495	196.1	244.3	203.7
500	196.2	245.4	203.8
505	196.3	246.6	204.0
510	196.5	247.7	203.1
515	196.6	248.8	203.2
520	196.8	250.0	203.4
525	196.9	250.1	203.5
530	197.0	250.3	203.7
535	197.1	251.4	203.8
540	197.3	252.5	202.9
545	197.5	253.7	203.1
550	197.7	253.9	204.3
555	197.8	255.0	204.4
560	197.9	255.1	204.5
565	198.1	256.3	204.7
570	198.3	256.5	203.9
575	198.4	256.7	204.1
580	198.6	256.8	205.2
585	198.7	257.9	205.3
590	198.9	259.1	204.5
595	199.0	260.3	204.7
600	199.1	261.4	204.8
605	199.3	261.5	204.9
610	199.5	262.7	205.1
615	199.5	262.7	205.1

Table 12-Experimental data for the runs with pressure varying at 10, 20, 25, and 30psig- Back pulsing duration and frequency fixed at 30 s.

Time (S)	10 psi	15 psi	20 psi	25 psi	30 psi
15	0.1	0	0	0	0.1
20	21.1	23.5	7.2	0	0
25	37.8	44	21.2	14.4	17.4
30	68.6	66.7	56.2	41.5	59.4
35	70.5	67.7	58.3	49.1	63.1
40	70.6	68	58.5	50.1	63.8
45	70.7	68	58.6	50.3	63.9
50	70.7	68	58.6	50.5	64.1
55	70.6	68	58.6	50.6	64.2
60	70.5	68	58.6	50.7	64.2
65	70.4	73	58.7	50.7	64.5
70	73.5	78.2	61.7	53	69.4
75	77.2	82.7	67.4	56.8	74.1
80	80.2	86.2	71.7	56.9	77.8
85	82.7	88.1	75.5	58.7	80.7
90	88.7	102.4	99.2	84.5	90.2
95	90	103.2	101	84.5	91.2
100	90.4	103.5	101.3	81.6	91.8
105	90.5	103.6	101.4	82.1	92
110	90.6	103.6	101.4	82.2	92.1
115	90.7	103.7	101.5	82.2	92.2
120	90.5	103.7	101.5	82.3	92.2
125	90.9	103.7	101.5	82.3	92.3
130	92.6	103.7	101.5	82.3	92.3
135	94	103.7	101.5	82.3	92.4
140	95.5	103.7	101.5	82.3	94.6
145	96.7	102.8	101.5	83	96.6
150	104.2	117.9	126.3	94.2	104.3
155	105.6	118.8	127.8	96	105
160	105.9	119	128.1	96.6	105.6
165	106.1	119.2	128.2	96.8	105.7
170	106.1	119.2	128.2	96.9	105.9
175	106.2	119.3	128.2	96.9	105.9
180	106.1	119.3	128.2	97	106
185	106.1	119.3	128.2	97	106
190	106.1	119.3	128.2	97	106.1
195	106.1	119.3	128.2	97.1	106.1
200	106.1	119.3	129.6	97.1	106.1
205	106.1	118.9	130	97.1	106.1
210	111.6	130.2	143.1	104.9	113

215	112.7	130.9	144.5	106.3	114
220	113	131	144.8	107	114.6
225	113.2	131.1	144.9	107.2	114.8
230	113.2	131.2	145	107.3	114.9
235	113.3	131.2	145.1	107.4	114.9
240	113.2	131.2	145.1	107.4	115
245	113.2	131.2	145.1	107.5	115.1
250	113.2	131.2	145.1	107.5	115.1
255	113.2	131.2	145.1	107.5	115.1
260	113.3	131.2	145.1	107.6	115.1
265	113.3	131.3	145.1	107.6	115.2
270	116.9	138.6	155	112.2	120.9
275	117.7	139.3	156.5	114.8	121.7
280	118.1	139.5	156.8	115.5	122.2
285	118.2	139.5	157	115.7	122.4
290	118.3	139.6	157.1	115.8	122.6
295	118.3	139.7	157.1	115.9	122.7
300	118.3	139.6	157.2	116	122.7
305	118.3	139.7	157.2	116	122.8
310	118.3	139.7	157.3	116.1	122.8

Table 13-Experimental data for the runs with back pulsing frequency varying at 30, 45, 60, and 75 s- Back pulsing pressure fixed at 20 psig and duration fixed at 30 s.

Time	30s	45s	60s	75s
15	0	0.1	0	6.1
20	7.2	30.5	7.3	38.9
25	21.2	54.8	27.8	61.3
30	56.2	62.4	38.7	68.8
35	58.3	71.2	45.5	75.2
40	58.5	97	51.4	81.4
45	58.6	96.8	56.2	86.2
50	58.6	96.8	66.9	89.7
55	58.6	96.2	97.9	93.1
60	58.6	96.2	98.6	95.9
65	58.7	96.1	98.9	98.3
70	61.7	97.1	99	113.7
75	67.4	97.1	99.1	124.5
80	71.7	97	99.1	125.2
85	75.5	96.9	99.1	125.3
90	99.2	97.9	99.2	125.4
95	101	96.8	99.2	125.4
100	101.3	98.3	99.1	125.4
105	101.4	100.5	99.1	125.4
110	101.4	101.2	100.3	125.4
115	101.5	115.3	102.5	125.4
120	101.5	114.9	104.7	125.4
125	101.5	115	106.8	128.1
130	101.5	115	108.1	128
135	101.5	115	108.4	121.3
140	101.5	115	108.6	123.6
145	101.5	115.8	116.4	125.4
150	126.3	115.7	117	126.9
155	127.8	115.7	117.3	128.3
160	128.1	115.6	117.4	130.3
165	128.2	115.6	117.5	131
170	128.2	115.6	117.6	131.8
175	128.2	115.5	117.7	159.1
180	128.2	115.5	117.7	158.1
185	128.2	115.5	117.7	158.5
190	128.2	124.3	117.7	158.5
195	128.2	123.9	117.6	158.5
200	129.6	124	117.7	158.4

205	130	124.1	117.7	158.4
210	143.1	124.1	117.7	158.4
215	144.5	124	117.7	158.4
220	144.8	124.7	117.7	158.4
225	144.9	124.6	117.7	158.4
230	145	124.7	117.7	158.4
235	145.1	124.6	123.6	158.4
240	145.1	124.6	124.1	158.5
245	145.1	124.6	124.4	159.8
250	145.1	124.6	124.6	161
255	145.1	124.5	124.7	162.2
260	145.1	124.5	124.7	163.2
265	145.1	132.3	124.8	164.3
270	155	132	124.8	165.3
275	156.5	132.1	124.8	166.2
280	156.8	132.2	124.8	175.3
285	157	132.2	124.8	176.4
290	157.1	132.2	124.8	177.1
295	157.1	132.4	124.8	177.4
300	157.2	132.7	124.9	177.5

Table 14- Experimental data for the runs with back pulsing frequency varying at 30, 45, 60, and 75 s- Back pulsing pressure fixed at 20 psig and duration fixed at 30 s; Repetition 2.

Time	30s-1	45s-1	60s-1	75s-1
15	0	0	0	0.1
20	15.3	24.7	21.6	24.3
25	24.8	45.2	38	41.7
30	56.4	56.5	48.3	52.1
35	57	63.9	54.9	58.9
40	57.5	69.5	60.4	64
45	57.8	99.5	64.8	67.7
50	57.9	100	68.4	71.2
55	58	100.4	71.6	74.2
60	58.1	100.6	94.3	78.9
65	58.2	100.8	94.4	86.9
70	58.3	100.8	94.7	88.4
75	58.4	100.9	94.8	48.5
80	59	101	94.8	103.3
85	61.6	101.1	94.9	103.4
90	87	104.7	94.9	103.4
95	87.2	108.3	94.9	103.4
100	87.5	111.7	95	103.4
105	87.7	114.6	95	103.5
110	87.9	117.1	95	103.3
115	87.9	119.6	97	103.4
120	88	134.9	100	103.4
125	88	135.1	102.9	103.4
130	88.1	135.5	105.7	103.5
135	88.1	135.8	108.2	103.5
140	88.2	135.9	110.8	104.6
145	88.2	136	113.1	107.6
150	102.2	136.1	125.9	110.6
155	102.6	136.1	126.4	113.4
160	103	136.2	126.8	116.1
165	103.2	136.3	127	116.8
170	103.3	136.2	127.1	117
175	103.4	136.3	127.1	117.1
180	103.5	136.4	127.3	132.2
185	103.5	136.4	127.3	132.1
190	103.6	136.5	127.4	132.3
195	103.6	156.2	127.4	132.4
200	103.7	156.4	127.4	132.5
205	103.8	156.7	127.5	132.6
210	114.2	156.9	127.4	132.6

215	114.3	157	127.5	132.6
220	114.7	157.1	127.5	132.7
225	114.8	157.2	127.6	132.7
230	115	157.2	128.8	132.7
235	115.1	157.2	130.9	132.8
240	115.1	157.3	151.6	132.8
245	115.2	157.3	151.7	132.8
250	115.2	157.4	152	132.9
255	115.3	157.4	152	132.8
260	115.3	157.4	152.2	132.9
265	115.4	157.4	152.2	132.9
270	123.4	177.9	152.3	132.9
275	123.6	178.3	152.3	133
280	123.9	178.7	152.3	133
285	124.1	178.9	152.3	152.8
290	124.3	179	152.3	152.5
295	124.4	179.1	152.2	152.7
300	124.4	179.2	152.2	152.7

Table 15- Back pulsing duration varying at 30, 45, 60, and 75 s- Back pulsing pressure fixed at 20 psig and frequency fixed at 30 s; Repetition 1.

Time (S)	30s-1	45s-1	60s-1	75s-1
15	4	0.9	0.4	0.3
20	4.2	20.5	14	20.7
25	9.7	50.1	44.6	45.4
30	20.6	70	68.5	63.4
35	28.6	80.2	82.7	73.1
40	32.2	88.4	90.6	80.5
45	35.3	95	98.9	87.7
50	37.8	100.9	104.5	90.7
55	40.2	106.4	109.7	91.1
60	42.3	110.2	113.9	91.4
65	44.2	111	117.7	95.5
70	46.1	111.3	120.9	99.9
75	68.8	128.8	134.5	108.5
80	68.9	130.6	137	109.9
85	69.1	131	137.4	110.4
90	69.3	131.3	137.6	111
95	69.4	131.4	137.7	111.4
100	69.4	131.5	137.6	111.6
105	69.4	131.6	137.8	111.8
110	69.6	131.7	137.8	112
115	69.5	131.7	137.8	112.2
120	69.6	131.8	137.9	112.3
125	69.6	131.8	138	112.4
130	69.7	131.9	137.8	112.5
135	69.7	132	137.9	112.6
140	69.7	135.5	137.9	112.7
145	69.7	140.8	137.9	112.8
150	69.7	145.4	137.9	112.7
155	69.7	149.7	138	112.8
160	70.1	153.9	138	112.8
165	71.5	156.1	138.6	112.9
170	72.7	156.5	143.1	115.2
175	73.9	156.7	147.2	119.8
180	85.5	156.8	151.4	124.1
185	86	157	152.9	128
190	86.2	157.1	153.4	131.6
195	86.4	174.6	153.6	134.7
200	86.4	176	153.5	137.8
205	86.5	176.3	153.7	140.9
210	86.5	176.4	166	143.7

215	86.6	176.5	169	144.5
220	86.6	176.6	169.3	144.7
225	86.7	176.6	169.6	153.6
230	86.7	176.7	169.7	154.7
235	86.7	176.7	169.8	155.3
240	86.7	176.7	169.6	155.5
245	86.8	176.8	169.8	155.8
250	86.8	176.8	169.8	155.9
255	86.8	176.8	170	156
260	86.8	176.8	169.9	156
265	86.8	176.9	169.9	156.2
270	86.9	176.9	170.2	156.3
275	86.9	176.9		156.3
280	86.9	180.2		156.4
285	99.3	184.4		156.4
290	99.7	187.9		156.6
295	99.9	188.6		156.5
300	100.1	188.8		156.6
305	100.2	189.1		156.7
310	100.3	189.2		156.8

Table 16- Back pulsing duration varying at 30, 45, 60, and 75 s- Back pulsing pressure fixed at 20 psig and frequency fixed at 30 s; Repetition 2.

Time (S)	30s-2	45s-2	60s-2	75s-2
15	-0.2	-1	0	0
20	-0.3	9.4	0.2	0
25	11.1	19.3	9	5
30	18.1	22.3	14	9.2
35	23.3	25.7	16	12.2
40	27.3	29.8	20.2	14.6
45	30.6	33.5	23.1	16.8
50	33.3	36.5	25.7	18.7
55	35.5	39.2	28.1	20.3
60	37.6	41.7	30.1	21.9
65	39.5	44	31	23.3
70	41.4	46.2	33.4	24.8
75	48.4	56.9	40.4	36.9
80	50.5	57.1	40.7	37.7
85	50.8	57.4	41	38.2
90	51	57.5	41.1	38.5
95	51.1	57.7	41.2	38.7
100	51.2	57.7	41.3	38.8
105	51.3	57.8	41.3	38.9
110	51.2	57.8	41.3	39
115	51.2	57.8	41.4	39.1
120	51.3	57.9	41.4	39.2
125	51.3	57.9	41.4	39.2
130	51.3	57.9	41.4	39.3
135	51.3	57.9	41.5	39.3
140	51.3	57.9	41.5	39.4
145	51.2	57.9	41.4	39.4
150	51.2	57.9	41.5	39.5
155	51.1	57.9	41.5	39.5
160	51.9	57.9	41.5	39.6
165	53.2	57.9	41.6	39.6
170	54.3	58	41.6	39.7
175	55.3	59.6	41.6	39.7
180	68.9	61.2	41.6	39.7
185	71.5	62.8	41.6	39.8
190	71.7	64.3	41.6	39.8
195	71.9	82	41.6	39.8
200	72	82.5	41.6	39.8
205	72	82.9	41.7	39.9
210	71.9	83	51.7	39.9

215	72	83.1	52.6	40
220	72	83.2	53.2	40
225	71.7	83.3	53.5	53.6
230	72	83.3	53.6	54.3
235	71.9	83.4	53.9	54.8
240	71.9	83.4	53.9	55
245	71.9	83.4	54	55.2
250	72	83.4	54.1	55.3
255	72	83.4	54.2	55.4
260	72	83.4	54.2	55.5
265	71.9	83.4	54.3	55.6
270	71.9	83.4	54.4	55.6
275	71.9	83.4	54.4	55.7
280	71.9	83.5	54.4	55.8
285	85.7	83.5	54.5	55.8
290	88.2	83.4	54.5	55.9
295	88.4	83.4	54.5	55.9
300	88.6	83.4	54.6	55.9
305	88.7	83.5	55.9	55.9
310	88.7	84.9	56	56

Bibliography

Abdelrasoul Amira [et al.] Gas and liquid backwash for flux restoration in latex paint effluent ultrafiltration [Journal] // Separation and Purification Technology. - 2018. - Vol. 204. - pp. 243-254.

Akhondi Ebrahim, Wicaksana Filicia and Fane Anthony Gordon Evaluation of fouling deposition, fouling reversibility and energy consumption of submerged hollow fiber membrane systems with periodic backwash [Journal] // Journal of Membrane Science. - 2014. - Vol. 452. - pp. 319-331.

Basile Angelo, Cassano Alfredo and Rastogi Navin K. Advances in Membrane Technologies for Water Treatment [Book]. - [s.l.] : Woodhead publishing Elsevier, 2015.

Bessiere Y. [et al.] Coupling air-assisted backwash and rinsing steps: a new way to improve ultrafiltration process operation for inside-out hollow fibre modules [Journal] // Desalination. - 2009. - Vol. 240. - pp. 71-77.

Cabassuda C [et al.] Air sparging in ultrafiltration hollow fibers: relationship between flux enhancement, cake characteristics and hydrodynamic [Journal] // Journal of Membrane Science. - 2001. - 1 : Vol. 181. - pp. 57-69.

Cui Z.F., Changb S. and Fane A.G. The use of gas bubbling to enhance membrane processes [Journal] // Journal of Membrane Science. - 2003. - Vol. 221. - pp. 1-35.

Fouladitajara Amir [et al.] Gas sparging to enhance permeate flux and reduce fouling resistances in cross flow microfiltration [Book]. - [s.l.] : Journal of Industrial and Engineering Chemistry, 2014.

Fujioka Takahiro and Nghiem Long D Fouling control of a ceramic microfiltration membrane for direct sewer mining by backwashing with ozonated water [Journal] // Separation and Purification Technology. - 2015. - Vol. 142. - pp. 268-273.

Gao Wei and Liang Heng Membrane fouling control in ultrafiltration technology for drinking water production: A review [Journal] // Desalination. - 2011. - Vol. 272. - pp. 1-8.

Hoek Von E. M. V and Tarabara V. V Encyclopedia of Membrane Science and Technology [Book]. - [s.l.] : Wiley. - Vol. Vol. 3.

Hoek Von E. M. V. and Tarabara V. V. Encyclopedia of Membrane Science and Technology [Book]. - [s.l.] : Wiley, 2013. - Vol. Vol. 3.

Jørgensen Camilla Elis [et al.] Optimization of protein fractionation by skim milk microfiltration: Choice of ceramic membrane pore size and filtration temperature [Journal]. - [s.l.] : Journal of Dairy Science, 2016. - 8 : Vol. 99.

Julian Helen [et al.] Scaling mitigation in submerged vacuum membrane distillation and crystallization (VMDC) with periodic air-backwash [Journal] // Journal of Membrane Sience. - 2018. - Vol. 547. - pp. 19-33.

Kim Jong-Oh [et al.] Effect of fouling reduction by ozone backwashing in a microfiltration system with advanced new membrane material [Journal] // Desalination. - 2007. - Vol. 240. - pp. 361-368.

Li Q.Y [et al.] Enhancement of ultrafiltration by gas sparging with flat sheet membrane modules [Journal] // Separation and Purification Technology. - 1998. - Vol. 14. - pp. 79-83.

Li Q.Y [et al.] Enhancement of ultrafiltration by gas sparging with flat sheet membrane modules [Journal]. - [s.l.] : Separation and Purification Technology, 1998. - 1-3 : Vol. 14.

Luo Jianquan [et al.] A two-stage ultrafiltration and nanofiltration process for recycling dairy wastewater [Journal] // Bioresource Technology. - [s.l.] : Bioresource Technology, 2011. - pp. 7437–7442.

Mercier-Bonin M, Lagane C and Fonade C Influence of a gas/liquid two-phase flow on the ultrafiltration and microfiltration performances: case of a ceramic flat sheet membrane [Journal] // Journal of Membrane Science. - 2000. - 1 : Vol. 180. - pp. 93-102.

Montgomery Douglas C. and Runger George C. Applied Statistics and Probability for Engineers Third Edition [Book]. - [s.l.] : John Wiley & Sons, Inc., 2003.

Myers Raymond H., Montgomery Douglas C. and Anderson-Cook Christine M. Response Surface Methodology: Process and Product Optimization Using Designed Experiments [Book]. - [s.l.] : Wiley-Blackwell, 2016.

Park Jin Yong, Choi Sung Jin and Park Bo Reum Effect of N2-back-flushing in multichannels ceramic microfiltration system for paper wastewater treatment [Journal] // Desalination. - 2007. - 202. - pp. 207–214.

Serraa Christophe [et al.] Use of air sparging to improve backwash efficiency in hollow-fiber modules [Journal] // Journal of Membrane Science. - 1999. - Vol. 161. - pp. 95-113.

Tangab Shengyin, Zhang Zhenghua and Zhang Xihui Coupling in-situ ozonation with ferric chloride addition for ceramic ultrafiltration membrane fouling mitigation in wastewater treatment: Quantitative fouling analysis [Journal] // Journal of Membrane Science. - [s.l.] : Elsevier, 2018. - Vol. 555. - pp. 307-317.

Visvanathan C. [et al.] Application of air backflushing technique in membrane bioreactor [Journal] // Water Science and Technology. - 1997. - 12 : Vol. 36. - pp. 259-266.

Wenten I G. Ultrafiltration in water treatment and its evaluation as pre-treatment for reverse osmosis system [Report]. - Indonesia : [s.n.].

Ye D, Saadat-Sanei S and Bérubé P.R Pulse bubble sparging for the control of hydraulically reversible fouling in submerged hollow fiber membrane systems [Journal] // Separation and Purification Technology. - 2014. - Vol. 123. - pp. 153-163.

Z.Abdullah Syed, R.Bérubé Pierre and J.Horne Derrick SEM imaging of membranes: Importance of sample preparation and imaging parameters [Journal] // Journal of Membrane Science. - 2014. - Vol. 463. - pp. 113-125.

Zhanga Wenxiang [et al.] Membrane cleaning assisted by high shear stress for restoring ultrafiltration membranes fouled by dairy wastewater [Journal] // Chemical Engineering Journal. - 2017.

Zielińska Magdalena and Galik Maciej Use of Ceramic Membranes in a Membrane Filtration Supported by Coagulation for the Treatment of Dairy Wastewater [Journal] // Water Air Soil Pollut. - 2017.